

## REVIEW

[View Article Online](#)  
[View Journal](#) | [View Issue](#)Cite this: *J. Mater. Chem. A*, 2024, **12**, 20606

## Flexible electrode materials for emerging electronics: materials, fabrication and applications

Kai Liu,<sup>a</sup> Tianyi Duan,<sup>a</sup> Fengran Zhang,<sup>a</sup> Xiaozhu Tian,<sup>a</sup> Hui Li,<sup>a</sup> Min Feng,<sup>b</sup> Rui Wang,<sup>\*c</sup> Benshuai Jiang<sup>c</sup> and Kewei Zhang<sup>ib</sup> <sup>\*a</sup>

With the swift evolution of smart products, flexible electronics characterized by their light weight, high flexibility and superior extensibility are becoming more and more fashionable in our daily life. As the foundational elements of flexible electronics, flexible electrodes have made a big splash in recent years in diverse fields of brain–computer interfaces, touch-screen displays, intelligent robots, and wearable and implantable devices. In this context, we analyzed the development of flexible electrode materials for electronics in the last 10 years by literature visualization. Our central emphasis is on all aspects of flexible electrodes, with a primary focus on flexible substrates (hydrogel/aerogel, fiber/fabric, polymer films) and active materials (metal and derivatives, carbon-based materials, MXenes, MOFs, etc.). Further, we extensively discuss the manufacturing methods of flexible electrodes, involving printing, vacuum filtration, deposition, electro/chemical plating, and others. The flexible electrodes have the potential to address a wide range of applications in flexible sensors, energy storage, and healthcare. Overall, the major challenges and future aspects of flexible electrodes are discussed for fabricating a new generation of flexible electronics.

Received 24th March 2024

Accepted 1st July 2024

DOI: 10.1039/d4ta01960a

[rsc.li/materials-a](https://rsc.li/materials-a)

## 1. Introduction

Flexible electronics is an emerging technology for manufacturing organic or inorganic materials on flexible or ductile substrates. Compared with traditional electronics, flexible electronics can be bent, folded, compressed, stretched, or even morphed into arbitrary shapes but still maintain stability, reliability, and integration, and have a more flexible environmental adaptability. In recent years, flexible electronic devices with good ductility and deformation resistance have attracted great attention and made great progress in personal healthcare, wearable energy storage, smart electronic skin (e-skin), and human–computer interaction (HCI).<sup>1,2</sup> The development of flexible electrodes has provided a great boost to the advancement of flexible technology, and is the key to solving problems such as continuous and stable signal acquisition. It is still a great challenge to fabricate flexible electronics with high toughness, light weight and good biocompatibility. The important factors affecting the performance of flexible electronics mainly come from the electrodes. Thus, the rational

design and fabrication of suitable flexible electrodes are critical.<sup>3,4</sup>

Flexible electrode materials for different applications require specific structures and properties, as they need to be integrated into various surfaces or folded and rolled for newly formed electronics. However, for practical applications, it is crucial to recognize the functional reliability of flexible electrode materials. The rapid development of nano-manufacturing has contributed to the boom in flexible electrode materials.<sup>5,6</sup> The fabrication of flexible electrodes in the traditional sense relies mainly on conductive flexible substrates, *e.g.* conductive fibers/fabrics,<sup>7</sup> hydrogels/aerogels,<sup>8</sup> polymer films,<sup>9</sup> *etc.* These flexible substrate-based stand-alone electrodes don't need to be loaded or doped with other functional materials. By virtue of their conductive, porous and flexible properties, they can be used independently as electrodes for flexible devices. The preparation method and device structure are relatively simple, suitable for large-area synthesis, wide source of materials, low cost, and good environmental friendliness, which has attracted much attention in the field of healthcare. However, these electrodes are: (i) large in size, poor in portability, and unfavorable for later integration; (ii) limited in application due to their own poor mechanical properties; and (iii) poor in conductivity and unstable in signal transmission.

Composite electrodes based on nano-functional materials refer to flexible electrodes with excellent interface contact and signal stability obtained by layer-by-layer assembly of functional materials such as carbon,<sup>10</sup> metals,<sup>11</sup> metal oxides,<sup>12</sup>

<sup>a</sup>State Key Laboratory of Bio-Fibers and Eco-Textiles, Collaborative Innovation Center for Marine Biomass Fibers, Materials and Textiles of Shandong Province, College of Materials Science and Engineering, Institute of Marine Biobased Materials, Qingdao University, Qingdao 266071, P. R. China. E-mail: zhkw@qdu.edu.cn

<sup>b</sup>College of Chemistry and Chemical Engineering, Hexi University, Zhangye 734000, P. R. China

<sup>c</sup>China Ceramic Optoelectronics (Shandong) Co., Ltd, Linyi 276000, P. R. China

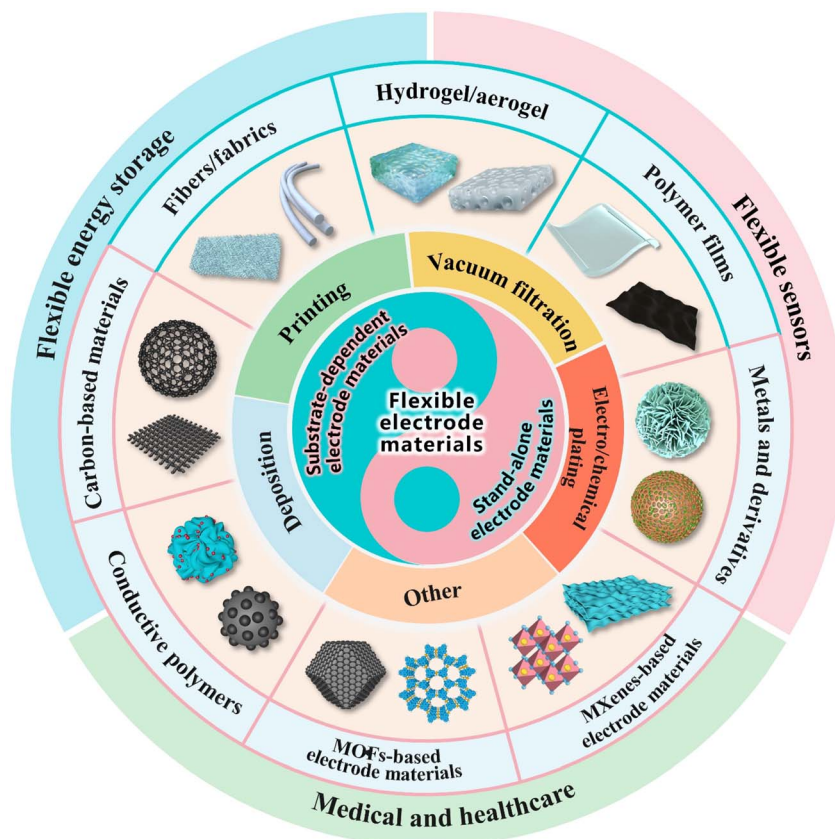


Fig. 1 Flexible electrode materials for emerging electronics: materials, fabrication and applications.

graphene,<sup>13,14</sup> MXenes,<sup>15</sup> MOFs,<sup>16</sup> *etc.*, with other flexible substrates. The outstanding advantage of this class of electrodes is that carrier transport at the interface is no longer limited, making the electrode conductive and signal transmission more stable and faster. However, the reproducibility is poor; in the repeated bending and folding process, the functional material easily breaks or detaches from the substrate, so the electric field distribution changes, which directly leads to signal interruption, resulting in electron and ion transmission being blocked, affecting the service life of flexible electronic devices. Besides, this type of preparation process is cumbersome and requires high-cost equipment, limiting its large-scale production.

With the continuous innovation of technology and in-depth research, people are constantly pioneering new flexible electrode design ideas and preparation methods. From new electronic materials to user-friendly electronic devices, it is expected that highly flexible, high-performance and high-stability electrodes can be designed through rational selection of functional materials and flexible substrates, as well as electrode preparation methods such as printing and vacuum filtration.<sup>17–19</sup> For example, Zhao *et al.*<sup>20</sup> chose polyurethane acrylate as a flexible substrate on which functional materials such as silver nanowires, gold, and platinum were deposited, and designed a platform device for fabricating elastic bioelectrodes based on microcracked conductive thin films, which has many

advantages such as being thin ( $\sim 140$  nm), soft ( $\sim 10$  MPa), stretchable ( $>150\%$ ), and highly conductive and comparable to that of clinically used rigid cuff electrodes with regard to their electrochemical and electrical properties. Zhang *et al.*<sup>21</sup> proposed a method to construct a soft ionic power supply on a micro-scale for the first time, using chemically active Ag/AgCl as the electrode material and hydrogel as the flexible substrate. The power supply can generate a current that lasts for more than 30 min, with a maximum output power of about 65 nanowatts and an endurance energy of up to 36 h. Kim and his team<sup>22</sup> synthesized a highly entangled hydrogel and elastomer, and a linear regression of the data estimated the fatigue threshold to be  $\sim 200$  J m<sup>-2</sup>. This value is about four times that of natural rubber, and about 20 times that of an ordinary hydrogel. The highly entangled elastomer has a fatigue threshold of  $\sim 240$  J m<sup>-2</sup>, which is much higher than those of conventional elastomers with similar stiffness, including neoprene, polydimethylsiloxane (PDMS), phosphonitrilic fluoroelastomers (PNF), and polyurethanes (PUs), which undoubtedly provides alternative materials for the selection of flexible substrates for flexible electrodes in the future. Consequently, through reasonable selection of electrode preparation methods, it can make the contact between the flexible substrate-functional material interface closer and less likely to fall off, and the signal collection is more stable, and has certain cost advantages.

vacuum filtration, deposition, electro/chemical plating, *etc.*, are also described in detail. We also discuss the latest progress of flexible electrode materials for application in the fields of flexible sensors, flexible energy storage, and medical and healthcare, which are currently in great demand.



In order to summarize the current research progress and development direction of flexible electronic devices and flexible electrode materials, we have summarized 21 595 publications on “flexible electronic devices” and 18 272 publications on “flexible electrode materials” in the past ten years, including papers, reviews, patents, conference proceedings, and dissertations (up to March 2024). As shown in Fig. 3a and b, publications related to flexible electronic devices and flexible electrodes are increasing year by year, showing an explosive trend in the last five years. This indicates that electronic devices are increasingly becoming flexible, and wearable and foldable devices are receiving more and more attention. Besides, China's attention to flexible devices is extremely high, being ranked first in the number of publications in the world, followed by the United States, South Korea, India and so on. With the fast development of wearable electronics in our lives, the attention to flexible electrode materials is increasing year by year, and the development prospect is broad.

### 3. Flexible substrates and active materials

According to the relationship between flexible substrates and active materials of electrodes, it can be divided into two main categories: (i) stand-alone electrode materials, where active materials are introduced into integrated electrodes inside flexible substrates; (ii) substrate-dependent electrode materials, where active materials rely on flexible substrates.

#### 3.1 Stand-alone electrode materials

**3.1.1 Hydrogel/aerogel.** Unlike other dry electrode materials, soft, moist and living biological tissues adhere more readily to the human body, facilitating the development of flexible and stable electronic devices. Hydrogel is a three-dimensional polymer network made of natural or synthetic materials with a water content of 70% to 90%, which is highly flexible, biocompatible and environmentally friendly. The softness and flexibility of hydrogels minimize their mechanical mismatch with biological tissues, and the high water content of hydrogels can provide a moist and ion-rich physiological environment. Due to their similarity to biological tissues and their versatility in electrochemistry, energy storage and bio-functional engineering, hydrogels have emerged as a promising electrode material for the next generation of flexible electronic devices.<sup>23,24</sup> However, pristine hydrogels often lead to poor performance in the existing flexible devices. Novel hydrogels with stable conductivity and superior sensing properties have been prepared by compositing with nanomaterials such as graphene and metal nanoparticles. Future innovations in hydrogel electrodes will require us to exploit the unique advantages of hydrogels based on a fundamental understanding of tissue–electrode interactions in order to rationally optimize various properties and parameters.

As shown in Fig. 4a, Han *et al.*<sup>25</sup> selected poly(vinyl alcohol) (PVA) and poly(vinylpyrrolidone) (PVP) to prepare hydrogel networks with a tissue-like modulus and good flexibility. The

integration of polydopamine (PDA) nanoparticles into hydrogels endowed them with high transparency, high self-adhesion and low impedance. The multichannel and wirelessly operated PVA–PVP–PDA hydrogel electrodes can establish conformal and stable interfaces with tissues, and exhibit high channel uniformity, low interfacial contact impedance, low power noise, long-term stability, and tolerance to sweat and motion. In addition, the hydrogel electrode-based system enables reliable and stable EEG signal acquisition and real-time display of the signals on a GUI *via* Bluetooth, demonstrating great potential applications in human consciousness assessment and multi-functional diagnostics. Hydrogels are soft in texture and have strong adhesion to brain tissues. Yan *et al.*<sup>29</sup> proposed a strategy to utilize a conductive adhesive hydrogel to mediate the treatment of traumatic brain injury (TBI). A hydrogel is prepared by combining cellulose nanowhiskers (PPCNW) coated with poly(3,4-ethylenedioxythiophene) (PEDOT) into a double cross-linked gelatin (dGel) network, which is expressed as PPCNW@dGel hydrogel. The PPCNW@dGel hydrogel can have good redox activity, electrical conductivity, softness, tissue adhesion and a modulus that matches that of the brain tissue. It was proved that the PPCNW@dGel hydrogel could protect the HT22 neuronal cells from excessive reactive oxygen species, and promote the proliferation, spreading and differentiation of HT22 neuronal cells under electrical stimulation. It can effectively prevent brain swelling/atrophy and inhibit the activation of astrocytes and microglia in brain tissue. In addition, the good electrical conductivity of the hydrogel provides a suitable physical microenvironment for neuronal growth, inhibits the damage of TBI to the hippocampus, and ultimately facilitates the recovery of neurological function after TBI. As flexible electrodes, hydrogels have made a big splash in the field of sensing, smart electronics and biomedicine. A variety of hydrogel-based flexible electrodes have been guaranteed to be bio-tissue compatible during short-term or one-time use. However, hydrogel electrodes are susceptible to massive water loss during long-term use, leading to electrode deformation and reduced signal acquisition capability, as well as skin inflammation induced by bacterial growth.<sup>30</sup> Therefore, there is an urgent need to develop new flexible bacteriostatic physiological electrode materials that can be used for long-lasting work in human–computer interfaces.

Aerogels with ultralight and extremely porous characters are showing great potential in absorption and sensor applications.<sup>31</sup> Wang *et al.*<sup>32</sup> successfully constructed a series of Ni/C@rGO composite aerogels (NCGCAs) with extremely high porosity through directional topological deformation of Ni-MOF and high-temperature pyrolysis. Due to its unique structural advantages, the NCGCAs aerogel not only increases electromagnetic energy consumption but also hinders heat conduction, and is becoming an excellent functional material for electromagnetic attenuation and thermal management. The prepared NCGCA-2 aerogel has a strong attenuation capability and matched impedance, showing its potential application in thermal management. Wang *et al.*<sup>26</sup> prepared long-lasting, lightweight and bacteriostatic aerogel electrodes based on degradable cellulose acetate composites by a thermally induced

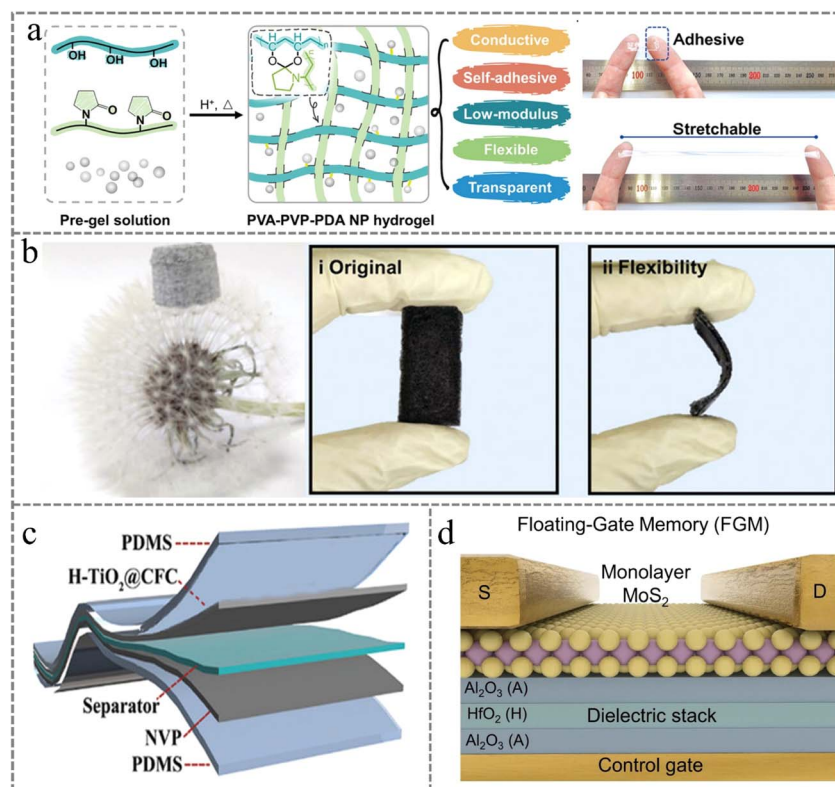


Fig. 4 (a) Hydrogel nanostructures for flexible self-adhesive electrodes and a physical picture. Reproduced with permission from ref. 25. Copyright©2023, Wiley. (b) Sponge-inspired flexible antimicrobial aerogel electrode. Reproduced with permission from ref. 26. Copyright©2024, Wiley. (c) Carbon fiber cloth supported flexible battery electrode. Reproduced with permission from ref. 27. Copyright©2020, Wiley. (d) Polymer film electrode. Reproduced with permission from ref. 28. Copyright©2024, Springer Nature.

phase separation technique (Fig. 4b). The aerogel electrode with great water absorption ( $\approx 800\%$ ) can be beneficial for intimate electrode–skin coupling and lower contact impedance. The doping of polypyrrole-coated silver nanowires ( $\text{AgNWs}@PPy$ ) enables the aerogel electrode to achieve more than 97.8% antimicrobial performance, and the compatibility with the skin allows it to work in clinical environments where the risk of bacterial infection is high. This one-pot thermally induced phase separation method simplifies the production and application of aerogel electrodes and facilitates large-scale production and practical applications.

**3.1.2 Fibers/fabrics.** With advances in nanotechnology and electroactive materials, traditional textiles have been transformed into a versatile platform for wearable electronics, which will inevitably drive the development of the next generation of flexible electronics. Flexible fibers/textiles are commonly used as substrate materials for making flexible electrodes, which are skin-friendly, multifunctional, and structurally tunable.<sup>33,34</sup> However, with continuous technological innovation, integrating functional particles (metals, carbon nanomaterials, *etc.*) into nanofibers or wrapping the functional layer materials on the surface can be made to give fibers/fabrics good conductivity and light transmittance without decreasing the flexibility and tensile properties, which can be directly used as a flexible electrode material, thus simplifying the way of personal interactive communication and portable sensing.<sup>35</sup> And its

preparation process is more mature and simple, has a good cost advantage, and is suitable for industrialized production.

Carbon fibers with high specific surface area, short ion diffusion paths and well-constrained electron transport paths are excellent choices for fabricating flexible energy storage electrodes. Carbon fibers with high electrical conductivity, good flexibility and large-scale preparation are considered promising electrodes for flexible EES devices. CC or carbon fabrics woven from carbon fiber bundles are also of interest for their high mechanical flexibility, high electrical conductivity, excellent thermal stability and considerable corrosion resistance.<sup>36,37</sup> Carbon fiber cloth is an ideal conductive substrate for flexible electrodes due to its high mechanical strength, high electrical conductivity, and low cost, and is widely used in the field of flexible lithium and sodium-ion batteries. Li *et al.*<sup>38</sup> proposed the use of a fiber cloth-loaded Ni–W–P alloy, and the expanded preparation of flexible Ni–W–P@HFC electrodes was achieved by doping W atoms in Ni–P alloy through a simple chemical plating method. The prepared electrodes exhibited excellent bifunctional activity and long-term stability, and DFT calculations revealed that the introduction of W into the Ni–P alloy lowered the reaction energy barrier. The Ni–W–P@HFC flexible electrode synthesized by the chemical plating method has interconnected fibers inside that help to form a good conductive network and a continuous electron transport path. Thanks to the regulation of fiber structure and doping control, the

prepared Ni–W–P@HFC electrodes have fast electron transfer capability and a large number of active sites, with excellent bifunctional activity and long-term stability. The large-scale preparation and solar-driven monolithic water decomposition of Ni–W–P@HFC flexible electrodes foretell a promising development prospect.

Electrical conductivity, mechanical flexibility, and large electroactive surface area are the most important factors in determining the performance of various flexible electrodes in energy storage devices. Woo *et al.*<sup>39</sup> reported a novel fiber-based layer-by-layer (LBL) assembly-induced metal electrodeposition method for the preparation of a variety of highly porous 3D current collectors with bulk metal-like conductivity, high flexibility, and large surface area. The method can address the shortcomings of previously reported methods by combining small molecule linker-mediated LBL assembly and metal electrodeposition. Moreover, this method is fully compatible with commercial plating processes and can therefore be directly extended to plating applications using a variety of other metals besides Ni. As shown in Fig. 4c, Wang *et al.*<sup>27</sup> used a hydrothermal-etching method to grow rutile titanium dioxide hollow matrices on carbon fiber cloth to construct an integrated electrode material (H–TiO<sub>2</sub>@CFC), which was applied to flexible sodium-ion batteries and exhibited excellent electrochemical performance at high multiplicity. The carbon fiber cloth not only enhances the electrical conductivity of the electrode, but also promotes the transport of sodium ions through its three-dimensional cross-linking architecture, and the TiO<sub>2</sub> hollow matrix can increase the contact between sodium ions and TiO<sub>2</sub> to shorten the sodium ion transport pathway. The flexible full battery assembled with this flexible composite electrode has excellent electrochemical performance and bending tolerance, which provides a feasible idea for the development of flexible energy storage devices for practical applications.

The use of flexible fibers/fabrics to provide the human body with electronic functionality that can collect, process, store, transmit and display information is an indispensable criterion for the future of flexible electronics.<sup>40</sup> Compared with complex and expensive electronic manufacturing processes, flexible fibers/fabrics are less expensive to produce, have great economic potential, and will inevitably drive the development of the next generation of flexible electronic products.

**3.1.3 Polymer films.** Polyimides (PIs) are common flexible insulating materials that are widely used as circuit components, electrical insulators, and power systems in modern electronic devices, large appliances, and aerospace applications due to their unique molecular structure and excellent electrical and thermal properties. In recent years, PIs have been widely used as artificial skin, flexible brain–computer interfaces, and other healthcare applications due to their unique biocompatibility, which allows them to follow tissue micro-movements without causing excessive inflammation. Wang *et al.*<sup>41</sup> chose a polyimide film as a flexible substrate and reported the development and application of a new doped super flexible neural (SUN) interface. Polyimide was chosen here because it is suitable for long-term neural implantation. This novel structure allows the SUN interface to deform in response to neural motion while utilizing

penetrating puncture electrodes for in-bundle recording. The novel 3D design integrates the tip structure for in-bundle nerve recording with an ultra-flexible substrate, enabling a unique conformal interface with the target nerve.

Polydimethylsiloxane (PDMS) is considered an ideal choice of substrate material because of its flexibility, stretchability, optical transparency, and biocompatibility, and because its Young's modulus is significantly lower than that of other commonly used materials. The long-term usability of PDMS-based bioelectronic devices in the *in vivo* environment has become important as more and more attention is being paid to implantable devices using soft, flexible and stretchable PDMS as a material. Electrocochography (ECoG) electrode arrays based on flexible materials are an excellent choice, especially polydimethylsiloxane (PDMS) materials. This material has better conformal contact implantation capabilities and its physical properties are close to those of biological tissues with less adverse effects on the tissues. However, realizing micron-sized electrodes on PDMS is a challenge. Moon *et al.*<sup>42</sup> performed an accelerated aging study based on ECoG electrode arrays of parylene-treated PDMS and for the first time evaluated in terms of stability and reliability over up to 8 months. The use of *p*-xylene-deposited PDMS and *p*-xylene-filled PDMS allowed the fabrication of soft, flexible and crack-free electrodes on PDMS substrates while maintaining their flexibility and stretchability properties. To evaluate the recording performance of the electrodes based on *p*-xylene-treated PDMS, the induced SEPs were further analyzed in terms of time–frequency analysis, amplitude, noise level, and signal-to-noise ratio. The *in vivo* experiments demonstrated that the developed PDMS-based ECoG arrays could chronically record SEPs for several months. Bao *et al.*<sup>28</sup> developed a neuromorphic electrical stimulation strategy (2D ES) based on an atomic-thickness MoS<sub>2</sub> floating-gate memory fork finger circuit (FGM IDC) (Fig. 4d). The device was based on a single-layer MoS<sub>2</sub> FGM IDC with a 2D ES control gate and Al<sub>2</sub>O<sub>3</sub>/HfO<sub>2</sub>/Al<sub>2</sub>O<sub>3</sub> stacked dielectrics sequentially deposited on a PI flexible substrate, overlaid with a single-layer MoS<sub>2</sub> film to form the IDC of neuromorphic ES and PDMS encapsulation layer. The 2D FGM IDC based on the MoS<sub>2</sub> monolayer serves as a neuromorphic stimulator that emits bionic stimulation spikes and can be electrically connected to flexible printed circuits and implantable flexible electrodes *via* an anisotropic conductive film and inserted into an adapter PCB for connection to an analyzer/monitor, promoting sympathetic release of norepinephrine, which inhibits cytokines associated with acute inflammation.

### 3.2 Substrate-dependent electrode materials

In addition to the stand-alone electrode materials that we introduced above, substrate-dependent electrode materials are developing more rapidly. They can integrate multiple advantages such as flexibility, stretchability, excellent electrical properties, and porosity. These electrodes are usually made of a substrate with a specific geometry and a functional material.<sup>43</sup> Typically, the stretchability mainly results from the structural deformation of the lower substrate, so that the upper rigid

material is subjected to negligible tensile stress. This prevents the fracture of the metallic material and ensures stable conductivity of the electrodes under tensile stress. The high performance comes from the functional materials constructed on the substrate.

### 3.2.1 Carbon-based materials

**3.2.1.1 Graphene and derivatives.** Graphene is an allotrope of carbon, consisting of a single layer of carbon atoms arranged in a hexagonal lattice. As a new type of two-dimensional carbon material with a single atomic layer thickness, graphene is unique for its excellent charge carrier mobility (conductivity of about  $1 \times 10^5 \text{ S cm}^{-1}$ ), high transmittance, large surface area, and remarkable chemical/thermal stability.<sup>44</sup> Notably, graphene has a Young's modulus of up to 1 TPa and a tensile strength of up to 130 GPa. It is considered to be an ideal material for transparent electrodes for next-generation wearable electronics, which can significantly improve the performance of electronic devices. In recent years, various methods have been successfully developed to synthesize graphene sheets, such as mechanical cutting, epitaxial growth, and chemical vapor deposition (CVD) to longitudinally cut CNTs into graphene, liquid-phase exfoliation of graphite into graphene, and reduced graphene. The indexes to evaluate the performance of graphene electrode materials mainly include film transmittance, electrical conductivity, substrate adhesion, time stability, surface roughness, work function, etc.

Graphene flexible electrode material preparation methods can be roughly categorized into dry and wet methods. The dry method is mainly based on the direct growth of ultrathin graphene films by the CVD method. Wet methods are mainly based on solution-processed graphene conductive inks, including RGO, and liquid-phase exfoliated graphene sheets.<sup>45</sup> Graphene-based materials currently applied to flexible electrodes can be broadly classified into zero-dimensional graphene quantum dots, one-dimensional graphene fibers, two-dimensional graphene flakes or films, and three-dimensional graphene-based foams and aerogels, as well as graphene complexes doped with other materials. Preparing high-performance flexible graphene-based electrode materials to meet the market demand and expanding the scope of use of graphene-based electrode materials are the focus of attention for flexible electronic devices nowadays.

Koo *et al.*<sup>46</sup> prepared graphene flexible novel transparent electrodes (PI@GR) for flexible organic solar cells using colorless polyimide (cPI) synthesized by polyamidoacetic acid (PAA) imidization, and employed cPI as a flexible substrate, achieving a photovoltaic conversion efficiency of 15.2%, which is the highest value reported so far for flexible organic solar cells (Fig. 5a). The multilayer graphene assembly with layers in close contact improves the adhesion between the electrode and the substrate and enhances the mechanical stability of the electrode. At the same time, the graphene electrode surface prepared by this method shows ultra-clean and ultra-smooth surface characteristics, with a light transmittance as high as 92% and a resistance as low as  $83 \Omega \text{ sq}^{-1}$ . The ultra-smooth electrode surface is also conducive to the reduction of interfacial defects in the cell, which can help the construction of high-

efficiency flexible organic solar cells. Dong *et al.*<sup>52</sup> introduced reduced graphene oxide (rGO) recording electrodes in the form of three-dimensional flexible films (rGO-3D) and two-dimensional films (rGO-2D), respectively, to obtain two different types of flexible graphene electrodes for long-term and acute recording. Porous rGO-3D electrodes suitable for permanent implantation and recording were made using typical vacuum filtration methods. Non-porous rGO-2D was prepared using coated rods for acute recording. This study not only provides new knowledge for balancing the conductivity and porosity of graphene oxide coatings, but also provides an in-depth evaluation of the physical and biological properties of this interface. Lee *et al.*<sup>53</sup> developed an ultrathin SEA neural probe ("NeuroWeb") composed of hexagonal boron nitride (h-BN) and graphene (Gr). Electrode pre-treatment was performed on a silicon substrate by spin-coating and photolithography, and then electroplating was utilized to form a highly roughened black platinum layer on the Pt surface to improve impedance. The device was fabricated using micro- and nanofabrication techniques, including photolithography, deposition, and electroplating steps, to achieve high-precision and high-quality device preparation.

**3.2.1.2 Carbon nanotubes (CNTs).** CNTs are a typical representative of carbonaceous nanomaterials with a large aspect ratio and high specific surface area, which have unique mechanical and electrical properties due to the nanoscale and quantum effects, can be integrated into flexible devices as 1D CNT fibers, 2D CNT membranes, and 3D CNT sponges in different forms, and have high electrical conductivity. With high conductivity, light weight and low cost, they are considered as an ideal material for the fabrication of flexible electrodes.<sup>54</sup> CNTs have a tensile strength of up to 63 GPa, which is 1000 times higher than that of copper wire. Theoretically, they are also considered one of the most promising flexible electrode materials for lightweight wearable electronic devices. CNTs can be categorized into two types, including SWCNTs and multi-walled CNTs (MWCNTs). Their synthesis methods mainly include: chemical vapor deposition, hydrothermal, electrostatic spinning, template method, etc. A 16-channel sensor array with suspended and decoupled mechanosensing elements, each made of an ultrathin CNT/PDMS nanocomposite sponge, was designed by Suo *et al.* and exhibited a wide detection bandwidth (Fig. 5b).<sup>47</sup> The device demonstrates real-time multi-channel motion recognition and human-computer interaction applications. The flexible sensing array can measure dynamic muscle deformation and EMG signals during muscle contraction. The multichannel design provides high spatial resolution and rich data information. This study provides an alternative to the traditional rigid measurement of EMG to achieve accurate capture of human movements, further broadening the scope of motion-interactive wearables in the upcoming era of the metaverse.

CNT network membranes have high mechanical strength, making it possible to form freestanding nanomembranes. However, CNT network membranes have a porous structure with large void areas, resulting in limited electrical coupling to neurons. Gao *et al.*<sup>55</sup> developed highly flexible and stretchable



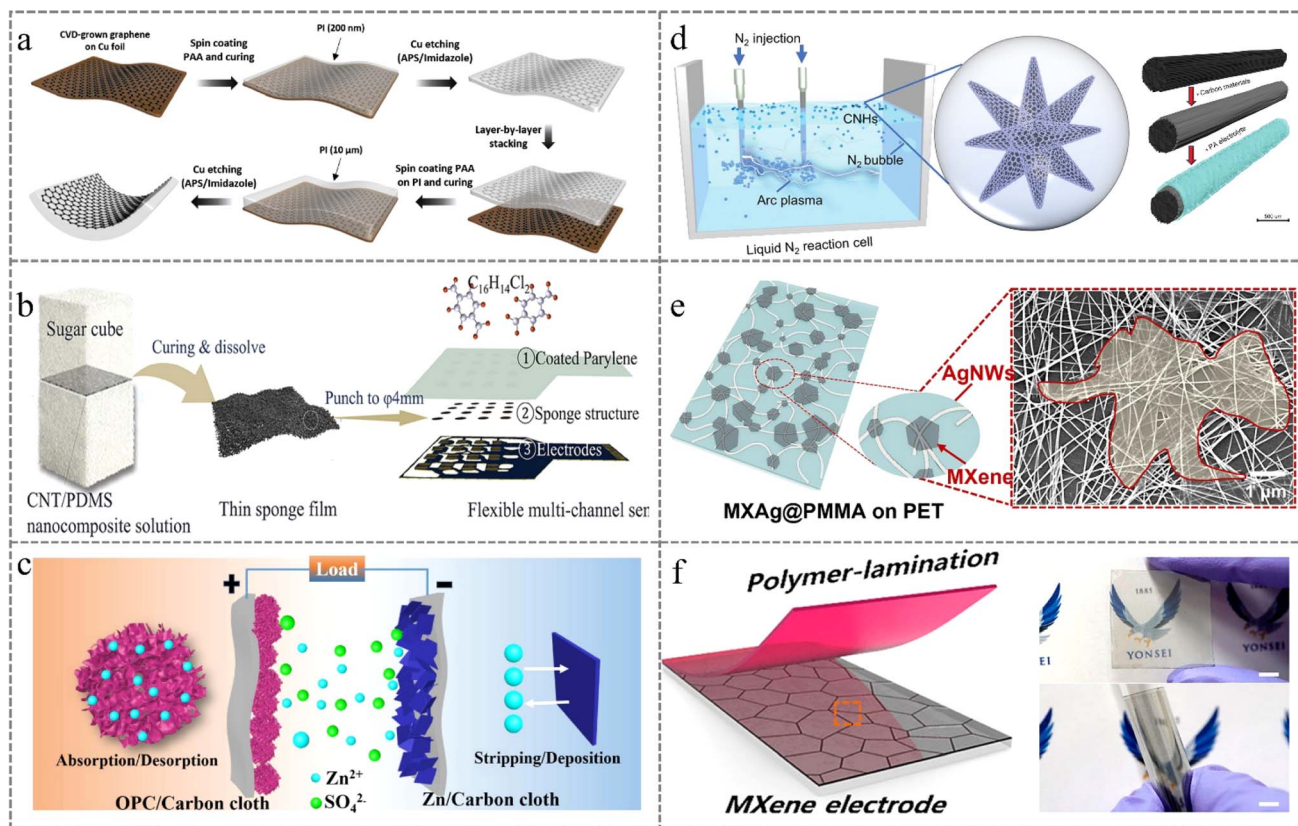


Fig. 5 (a) Graphene–polyimide composite flexible electrode. Reproduced with permission from ref. 46. Copyright©2020, Elsevier. (b) CNT/PDMS nanocomposite flexible electrode. Reproduced with permission from ref. 47. Copyright©2024, Wiley. (c) Flexible cathodes for zinc capacitors based on porous carbon materials. Reproduced with permission from ref. 48. Copyright©2020, Elsevier. (d) Asymmetric carbon nanohorns as electrodes for soft capacitors. Reproduced with permission from ref. 49. This is an open-access article. (e) MXene thin-film electrode. Reproduced with permission from ref. 50. Copyright©2022, American Chemical Society. (f) Polymer-encapsulated MXene thin-film electrode. Reproduced with permission from ref. 51. Copyright©2021, American Chemical Society.

graphene membrane microelectrode arrays (CeG-MEAs) for stable long-term neural recordings using stand-alone CeG as recording microelectrodes, and implantable neural probes consisting of robust carbon nanotube network-embroidered CeGs as stand-alone recording microelectrodes. CeG-MEAs are ultra-flexible and maintain their structural and electrical integrity under large mechanical deformations, thus enabling cell-scale electrode-tissue interfaces. The findings highlight the potential of ultra-flexible and freestanding carbon nanomembranes for stabilizing neural interfaces in the brain. CNTs are preferred for energy storage due to their large specific surface area (SSA) and pore size distribution (PSD) for capacity and efficiency enhancement. Kazari *et al.*<sup>56</sup> utilized multi-walled carbon nanotube arrays grown on stainless steel mesh using zero-oxidation state precursors and nitrogen plasma with *in situ* deposition of plasma-enhanced atoms of ruthenium as a flexible supercapacitor electrode. The functionalized CNTs contain carbonyl and carboxyl functional groups that contribute to film nucleation. The fabrication of 3D flexible supercapacitor electrodes by using this method does not require any binder components and solution-based synthesis steps and does not produce any toxic by-products.

**3.2.1.3 Porous and hollow carbon materials.** Rigid carbon materials are difficult to relieve the stress on the surface of the active material when acting as an electrode, leading to the occurrence of harmful reactions and poor performance. Porous and hollow carbon materials are characterized by large specific surface area, ordered pore size distribution, and controllable topology. These are usually prepared by pyrolytic activation, template method, *etc.* They are often used as electrode materials for energy storage devices such as wave absorbers, batteries and supercapacitors.

Zhou and his team<sup>57</sup> prepared N/P co-doped porous carbon materials with hierarchical structure using  $\text{Arg}[\text{H}_2\text{PO}_4]_2$  for flexible electrodes of high-performance supercapacitors. Due to the fast transport of electrolyte ions in the hierarchical porous structure, the prepared Arg-2-900 has a stable bilayer capacitance, with a specific capacitance retention of up to 94% after 10 000 cycles. In order to simultaneously satisfy the requirements of wearable electronics for high energy/power density, safety, and flexibility, Zheng *et al.*<sup>48</sup> synthesized a three-dimensional porous carbon material (PC) by a combustion method in a bottom-up manner, and subsequently immersed PC into concentrated nitric acid for oxidative etching to obtain oxygen-enriched 3D porous carbon (OPC) (Fig. 5c). The zinc



nanosheet anode and OPC cathode were integrated together to assemble a solid-state zinc ion capacitor (ZIC). Utilizing the pseudocapacitance provided by abundant oxygen-containing functional groups and the unique pore structure of the porous carbon to endow the cathode with fast electrochemical kinetic properties, the ZICs possessed an excellent specific capacity of  $132.7 \text{ mA h g}^{-1}$  at a current density of  $1.0 \text{ A g}^{-1}$ , an excellent  $82.36 \text{ W h kg}^{-1}$  energy density and good cycling stability of 87.6% over 10 000 cycles.

Xu *et al.*<sup>58</sup> prepared micro- and nano- $\text{NiS}_2/\text{C}$  materials from nickel salts and polyvinylpyrrolidone (PVP K30), and on the surface of micro- and nano- $\text{NiS}_2/\text{C}$  particles, a nanoscale flexible hollow carbon buffer layer (FHCBL) was synthesized by KOH activation and HCl etching. It is shown that the nanoscale flexible hollow carbon buffer layer can not only give full play to the porous carbon effect and improve the performance of supercapacitors, but also solve the problems of difficult filling of porous carbon composites and low quality of active materials, and this strategy can be applied to the successful fabrication of a wide range of high-performance energy storage and conversion devices. Hollow carbon-based wave-absorbing materials, as an alternative to graphene-based carbon materials, solves the problems of heavy mass and complicated preparation process of common wave-absorbing materials, and has the advantages of high stability, low reflection loss and long effective bandwidth. Inspired by the multiple reflections of hollow core-shell structures and the increased interfacial polarization of flower-like layered structures, Zhao *et al.*<sup>59</sup> prepared multilayered hollow carbon spheres/CF@ $\text{MoSe}_2$  with carbon fiber as the substrate, and introduced transition metal sulfides to coordinate the electromagnetic parameters. The specific morphology of the core-shell structure of the multilayered hollow carbon spheres plays a crucial role in the final absorption performance.

**3.2.1.4 Other carbon materials.** In addition to the common carbon materials summarized above, carbon materials such as fullerenes, carbon nanohorns, carbon spheres, and carbon nanofibers, which have remarkable structural and functional tunability,<sup>60</sup> are often used as electrode materials for flexible electronic devices.

Fullerenes and their derivatives are among the most widely used n-type materials in organic electronics because of their suitable energy level arrangement and superior electron mobility.<sup>61</sup> Martinez-Agramunt *et al.*<sup>62</sup> obtained palladium corner metal cubic arrays based on azocarbene (NHC) by using a metal-directed self-assembly strategy. The “cubic” cage has a cavity that makes it suitable for the encapsulation of fullerene  $\text{C}_{60}$  and  $\text{C}_{70}$ . The affinity of the cage molecules for larger fullerenes is higher than that of smaller fullerenes, allowing for the sieving of  $\text{C}_{70}$ . Zhang *et al.*<sup>63</sup> proposed a scalable approach to prepare flexible reduced graphene oxide/fullerene (RGO/ $\text{C}_{60}$ ) smart fibers using wet-spun assemblies of graphene oxide (GO) and hydroxylated fullerenes, which were chemically reduced.  $\text{C}_{60}$  interventions may result in the transformation of the RGO layer of the disordered structure to be transformed into an ordered structure. The introduction of zero-dimensional fullerene as a trapping agent into the reduced graphene oxide

fibers significantly improved the free radical trapping ability and the accessible surface area of the chemicals, which ultimately endowed the reduced graphene oxide fibers with electrocatalytic activity.

Carbon nanohorns (CNHs) are a special type of tapered carbon nanomaterial similar to carbon nanotubes (CNTs). With different dispersions, structural geometries, surface chemistries and synthesis methods, they are generally prepared by laser ablation, electric arc and Joule heating methods without the addition of metal catalysts,<sup>64</sup> and are characterized by high purity and environmental friendliness. As shown in Fig. 5d, Li *et al.*<sup>49</sup> prepared asymmetric single-walled carbon nanohorns (SWCNHs) by controlling the arc reaction at low temperature (77 K) and used them as an active material for the fabrication of flexible solid carbon filament electrochemical supercapacitors with high power density and ultra-low cutoff frequency. Toxicity of carbon nanomaterials is also a major constraint for their application in the biomedical field. Paneer Selvam and his team<sup>65</sup> prepared carbon nanohorn composites (CNH-cell) loaded with different concentrations of cellulose and verified their safety for human skin applications. The composites also have flexibility, strength, and electrical conductivity, which suggests that they have high potential in various modern applications.

Carbon nanofibers (CNFs) have become a hot research topic in the field of materials in recent years due to their easy processability and compatibility. Their preparation methods mainly include the electric arc method, template method, chemical vapor deposition, co-spinning and electrostatic spinning. When the fiber size is reduced from the conventional micrometer scale to the nanometer scale, the ultra-high specific surface area and abundant defect structure brought about by the diameter refinement can greatly improve the physicochemical properties of CNF films. Wang *et al.*<sup>66</sup> adjusted the preoxidation temperature, which led to a significant increase in the content of graphitized flakes in the carbonized CNFs. The prepared composite CNF films can be arbitrarily folded into any shape and can undergo thousands of dynamic bending deformation cycles. This strategy is used for scalable fabrication of filamentary flexible CNF films, which provides a universally effective strategy for the fabrication of truly foldable flexible CNFs. Li *et al.*<sup>67</sup> prepared  $\text{NiCo}_2\text{O}_4/\text{N}$ -doped flexible hollow carbon nanofiber ( $\text{NiCo}_2\text{O}_4/\text{HCNF}$ ) composites by using coaxial electrostatic spinning and hydrothermal synthesis with polyacrylonitrile-co-acrylamide as the precursor to construct the three-dimensional freestanding  $\text{NiCo}_2\text{O}_4/\text{HCNF}$  flexible electrodes for all-solid-state supercapacitors. And they were used as additive-free electrodes for all-solid-state supercapacitors. The hollow structure of HCNFs provided inner and outer surfaces for  $\text{NiCo}_2\text{O}_4$  nanosheets, which shortened the ion migration distance. The specific capacitance at  $1 \text{ A g}^{-1}$  was improved to  $1864.0 \text{ F g}^{-1}$ , and the capacitance retention was 99.2% after 1000 cycles, indicating its potential application in wearable and portable devices.

Carbon spheres (CSs) have become a current research hotspot in the field of flexible electronic devices due to their good electrical conductivity, large specific surface area, short charge

transport length, and high stacking density. Wang *et al.*<sup>68</sup> proposed a hydrothermal preforming process with pH adjustment before pyrolysis to synthesize MoO<sub>2</sub> composite structures of MoO<sub>2</sub>/CS with adjustable morphology. The composite structure can greatly improve the conductivity and structural instability of the material, resulting in a high theoretical capacitance. This work provides a new direction for the rational design of efficient composite electrode materials by adjusting the local structures of the guest and host materials. Zhao *et al.*<sup>69</sup> proposed a preparation method for the efficient growth of high-quality dense ZIF-67 layers on a flexible carbon foam (CF) three-dimensional skeleton using ALD pretreatment. During the subsequent pyrolysis process, the ZIF-67 layer was transformed into a porous layer consisting of carbon spherical particles (Co-N-CSs), which maintained a large specific surface area and a high pore volume. This work provides a strategy for the synthesis of MOF-based materials with potential for structural and methodological innovations, and the Co-N-CS-CF composite structure can be a new generation of flexible HER electrodes applied in the field of flexible devices.

**3.2.2 MXene-based electrode materials.** MXenes, a class of transition metal carbides, nitrides and carbonitrides collectively, have been widely studied in the application of flexible electronic devices.<sup>70,71</sup> As an emerging two-dimensional material, it has very excellent electrical conductivity, chemical activity, adsorption properties, *etc.*, as well as mechanical strength and flexibility, which makes MXenes have great potential for development in applications such as sensors, energy storage and conversion. MXenes have become one of the representative materials for flexible electrodes for electronic devices, but realizing highly transparent and conductive MXene electrodes for flexible photodetectors remains a challenge due to the trade-off between resistance and transmittance.<sup>72</sup> Chen *et al.*<sup>73</sup> developed a novel MXene/leaf composite highly transparent and conductive flexible electrode with a transmittance of up to 90% and a resistance of only 3  $\Omega$   $\text{aq}^{-1}$ . The MXene/leaf composite electrode was first obtained by using a poplar leaf vein stripped of its flesh as a support structure, which was prepared by the MILD method after coating multilayers of m-Ti<sub>3</sub>C<sub>2</sub>T<sub>x</sub> type MXene. Due to the large number of polar groups on the surfaces of both m-Ti<sub>3</sub>C<sub>2</sub>T<sub>x</sub> and poplar plum leaf veins, there is a strong interaction between m-Ti<sub>3</sub>C<sub>2</sub>T<sub>x</sub> and the leaf veins, which results in the composite electrode with excellent mechanical strength and flexibility. The UV detector prepared with the MXene/leaf composite electrode has sensitive photoresponsiveness and very good flexibility, and the photocurrent can be maintained at 90% of the original level after 1000 rounds of bending and curling, which shows great potential for future applications in the field of optoelectronics. Wang and his team<sup>74</sup> prepared a TENG-driven self-powered MXene/TiO<sub>2</sub>/SnSe sensor for SO<sub>2</sub> gas detection with excellent response, which is 14 times better than that of resistive sensors. The sensor signal can be transmitted to a smartphone and upper module to monitor environmental factors such as temperature, humidity, SO<sub>2</sub> concentration, and water surface height in real time. The back propagation neural network model was used to integrate and

process the data from the sensor system to achieve temperature and humidity error correction of the gas sensor.

Although transparent Ti<sub>3</sub>C<sub>2</sub>T<sub>x</sub> MXene electrodes with high conductivity are promising, their applicability to displays is still limited due to the high sheet resistance caused by thin sheet junctions and surface roughness. A flexible and transparent MXene-AgNW hybrid electrode for full solution processed QLEDs was demonstrated by Jiang *et al.*<sup>50</sup> (Fig. 5e). It consists of a highly conductive AgNW network mixed with solution-processed MXene flakes. Efficient welding of wire-to-wire joints using MXene flakes results in electrodes with low sheet resistance and high transparency. This solution-treated nanoconductor-based flexible transparent electrode with the tunable figure of merit provides a method for the development of emerging high-performance, wearable, and cost-effective soft electroluminescent devices. Lee *et al.*<sup>51</sup> reported a transparent and flexible MXene electronic device that is made by laminating a polymer film onto a solution-treated MXene layer to protect the MXene film from exposure to harsh environmental conditions (Fig. 5f). The electrode has excellent oxidation resistance and is suitable for use in a variety of electronic devices based on an electric field-driven process. This PL-MXene electrode was developed through a two-step spin-coating process that first prepares a thin and homogeneous MXene film, and second encapsulates the MXene film using a layer of insulating polymer film. It was shown that the polymer laminate encapsulation method on the MXene layer significantly improves the oxidation resistance of intrinsically transparent and conductive MXene electrodes, which will broaden their potential to be used as flexible and transparent electrodes in a wide range of wearable and repairable electronic products. A self-powered flexible humidity sensing device based on poly(vinyl alcohol)/Ti<sub>3</sub>C<sub>2</sub>T<sub>x</sub> (PVA/MXene) nanofiber films and a monolayer molybdenum diselenide (MoSe<sub>2</sub>) piezoelectric nanogenerator (PENG) was first reported by Wang *et al.*<sup>75</sup> The flexible PET substrate-based PVA/MXene nanofiber humidity sensor driven by a monolayer MoSe<sub>2</sub> PENG has a high response of  $\sim 40$ , a fast response/recovery time of 0.9/6.3 s, a low hysteresis rate of 1.8%, and good repeatability.

**3.2.3 Metals and derivatives.** Metals and their derivatives are mostly found in rigid solid form, but when small enough in size and thin enough in thickness, they can be implanted as electrodes in flexible electronic devices. Traditional metal electrodes are generally gold, silver, copper and other conductor materials, mainly used for electrodes and wires. For modern printing processes, conductive materials are mostly used as conductive nano-inks, including nanoparticles and nanowires. Nanoparticles of metals and their derivatives can be sintered into thin films or wires in addition to good conductivity.<sup>76,77</sup> Common metals and their derivatives that are directly used as flexible electrodes include gold/silver/copper nanoparticles, liquid metals (LMs), and transition metal oxides/sulfides/hydroxides.<sup>78</sup> The outstanding advantage of these electrodes is that the conductivity of the material does not degrade upon applying multiple cycles of certain stress ( $>1\%$ ), and they are widely used in the fields of sensors, energy storage devices, and so on.

**3.2.3.1 Metal nanoparticles.** Almost all conventional electronic systems rely on conducting materials such as metals, where free electrons act as mobile charge carriers. LMs are metals that are liquid near room temperature, also known as low melting point metals, such as gallium-based and bismuth-based metals and their alloys. Because of their fluidity, high electrical conductivity, unique phase transition and low toxicity, LMs are gradually becoming attractive electrode materials for modern flexible electronic devices. Others, such as mercury, cesium, and sodium-potassium alloys, are also in the liquid state at room temperature, but their applications are greatly restricted due to toxicity, radioactivity, and danger. Peng *et al.*<sup>79</sup> successfully constructed ultrasensitive, anisotropically conducting flexible electronic devices based on conductive biphasic LM-polymer composite gels. The anisotropic conductive gel (ACG) has an extremely low detection limit (strain: 0.01%, stress: 3 Pa) and excellent flexibility (elongation at break: 110%, modulus: 342 kPa). The local electrical conductivity due to the two-phase metal and insulating oxide particle structure gives the composites an anisotropic conductivity, and this conductive network is very sensitive to external forces. The relationship between the anisotropic structure, subtle vibrations and electrical properties has been thoroughly investigated through rheological-electrical experiments. The ACG can recognize

subtle strains and frequencies synchronously with 99% accuracy. In addition, the adhesive properties of the polymer gel allow ACGs to be integrated with existing rigid electronic devices for signal acquisition and conditioning. ACGs are ideal candidates for future advanced technologies such as human-computer interaction, smart robotics, and health management. ACGs can capture a wide variety of physiological information related to sleep, exercise, and surgical recovery monitoring. Multi-size universal self-assembly (MUS) of LM particles of various diameters (<500  $\mu\text{m}$ ) was realized by Li *et al.*<sup>80</sup> (Fig. 6a). Thanks to the shielding from gravitational interference and the help of the Marangoni force in the MUS method, nanometer to micrometer (<500  $\mu\text{m}$ ) LM particles can be self-assembled into monolayers in the air-water interface. The monolayers can be conformally transferred to complex surfaces such as silicon wafers, spherical surfaces, and human skin. This eliminates interference with the mechanical response of conventional substrates and makes LM electronic tattoos more user-friendly. Ultra-conformal LM monolayers provide a valuable tool for further research in conformal flexible circuits, wearable sensors and other device applications.

Mechanically transformed electronic systems (TESSs) constructed using metal particles are an innovative class of electronics due to their ability to switch between rigid and flexible

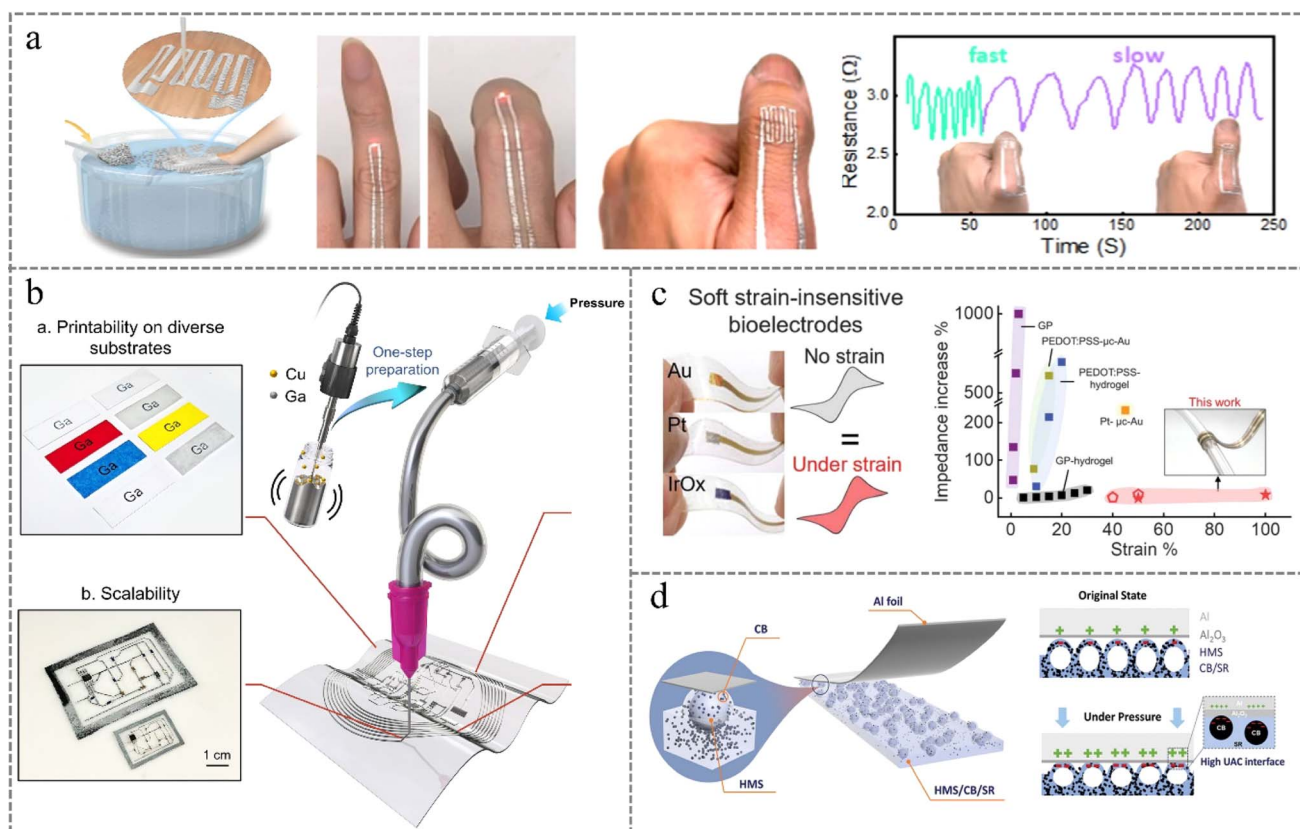


**Fig. 6** (a) LM particle monolayer flexible electrode. Reproduced with permission from ref. 80. Copyright©2023, Springer Nature. (b) Gallium–copper (Ga–Cu) composite ink flexible electrode. Reproduced with permission from ref. 81. This is an open access article. (c) Metal and metal oxide composite electrode. Reproduced with permission from ref. 82. Copyright©2022, American Association for the Advancement of Science. (d)  $\text{MnO}_2/\text{rGO}$  composite flexible electrode. Reproduced with permission from ref. 83. Copyright©2024, Wiley.



states, thus making flexible electronic devices more multi-applicable. However, the challenges posed by the high surface tension and low viscosity of metallic materials greatly hinder manufacturability. Kwon *et al.*<sup>81</sup> developed a stiffness-tunable gallium-copper (Ga-Cu) composite ink capable of fabricating complex, high-resolution TES circuits directly *via* 3D printing, providing high-resolution ( $\sim 50\ \mu\text{m}$ ) patterning, high electrical conductivity, and bi-directional soft-stiffness convertibility (Fig. 6b). The circuits can be used as both electronic layers and mechanical conversion frameworks. A low-copper strategy is used to rationally adjust the gallium-copper (Ga-Cu) ratio in the composite ink, and the product has a stiffness tuning ratio of 990 for  $150\ \mu\text{m}$  thick devices with high conductivity and high-resolution picturization. This work makes metal particle-based TES fabrication simple and versatile, opening up possibilities for wearables, implantable devices, consumer electronics and robotics.

**3.2.3.2 Transition metal compounds.** Transition metal compounds include metal oxides, metal sulfides, and metal hydroxides. These substances have lower electrical conductivity than metal particles, wider band gaps, and semiconductor properties. The common ZnO and ZnS have excellent piezoelectric properties;  $\text{SnO}_2$  and  $\text{In}_2\text{O}_3$  have high optical transparency; and indium tin oxide (ITO) films have excellent optical and electrical properties. They can be applied to pressure sensing, liquid crystal display and electrostatic shielding, solar cells, thermal management and other fields.<sup>84,85</sup> The most commonly used methods for preparing transition metal compounds are magnetron sputtering and electrochemical deposition. The interaction of electronics with biological tissues is fundamental for probing and driving biological systems. Clinically established bioelectronics-tissue interface materials with good electrochemical properties are rigid and brittle. Zhao *et al.*<sup>82</sup> designed a composite material with a stretchable, highly conductive and strain-insensitive layered structure for a bio-electrode with clinically determined brittle interface materials (iridium oxide, gold, platinum, and carbon) (Fig. 6c). At its core, the bioelectrode material configuration is decoupled into an interfacial element for electron transport and an interconnecting element for electron transport. The authors pair these bio-electrodes with different electrochemical probing methods (amperometric, voltammetric, and potentiometric) and demonstrate strain-sensitive sensing of a wide range of biomarkers and *in vivo* neuromodulation. The superior electrochemical stability of the various interfacial materials and the conductivity of silver nanowires were utilized without their inherent limitations in a stretchable bioelectronic environment.

In order to solve the problems of mechanical susceptibility and quantum tunneling in nanometer-thick dielectric layers, Yang *et al.*<sup>83</sup> utilized the natural oxide layer on the surface of aluminum as a nanoscale ultrathin dielectric layer, whereas a carbon black/silicone rubber (CB/SR) composite and aluminum were used as the upper and lower electrodes, respectively (Fig. 6d). The tunneling current at the  $\text{Al}_2\text{O}_3$  interface was effectively suppressed using the Schottky effect between CB with semiconducting properties and aluminum, and thus a unit-area capacitance (UAC) value of up to  $50\ \text{nF}$

$\text{cm}^{-2}$  was obtained at the ultrathin natural  $\text{Al}_2\text{O}_3$  interface. Based on this high UAC interface, the authors' team further proposed a flexible electrode microstructuring scheme with a hollow hemispherical morphology, and prepared flexible pressure sensors with sensitivities and linear intervals up to  $8.6\ \text{kPa}^{-1}$  and  $50\ \text{kPa}$ , respectively. This hollow hemispherical micro-structuring scheme on the surface of flexible electrodes enables the preparation of flexible pressure sensors with high sensitivity and wide linear intervals. Thanks to the excellent environmental stability and self-healing properties of the natural  $\text{Al}_2\text{O}_3$  layer, the flexible pressure sensors based on this design show excellent stability under different environmental and mechanical working conditions. Metal oxides have been investigated as representative pseudocapacitor materials for batteries due to their reversible redox reaction, high energy density and excellent specific capacitance. Huang *et al.*<sup>86</sup> prepared  $\text{MnO}_2/\text{rGO}$  electrodes by a vacuum filtration method, which were finally piggybacked into a rechargeable zinc-ion battery with high energy density and recyclability. The reason for its high performance is the fact that the high specific surface area of the  $\text{MnO}_2/\text{rGO}$  composite provides more active sites for lithium redox reactions, allowing full reaction with lithium ions, increasing capacity and improving rate capability. Notably, there is no adhesive between  $\text{MnO}_2$  and rGO, and this work opens up new ideas for powering next-generation flexible electronics.

**3.2.4 Conductive polymers.** Since their discovery in the 1960s, conducting polymers have attracted great interest in wearable smart devices due to their good tensile strength, high electrical activity, high flexibility, light weight and good processability compared to inorganic conducting materials. This class of materials is low-cost and environmentally friendly due to its unique multi-electronic response and structural and chemical versatility.<sup>87</sup> Some conducting polymer organics such as polyaniline (PANI), polypyrrole (PPy), poly(3,4-ethylenedioxythiophene) (PEDOT) and their derivatives have been investigated as electrode materials for flexible electronic devices. In humid physiological environments, the fragile interface between conducting polymers and electrodes greatly limits their use and reliability. Zhang *et al.*<sup>88</sup> prepared PEDOT:poly(SS-4VP) interpenetrating network hydrogels by chemically grafting a functional long-chain polymer (poly(styrenesulfonic acid-co-4-vinylpyridine) (poly(SS-4VP))) onto a metal substrate, electrochemically depositing conducting polymers (*e.g.*, PEDOT, *etc.*) and further chemical cross-linking (Fig. 7a). The PEDOT:poly(SS-4VP) interpenetrating network hydrogels were prepared. A versatile but reliable strategy was established to seamlessly connect conventional electrodes with conductive hydrogel coatings with tissue-like modulus, highly desirable electrochemical properties, robust interfaces and long-term reliability. Numerical simulations reveal the synergistic effects of toughening mechanisms, covalent anchoring of long-chain polymers, and chemical cross-linking in enhancing the long-term stability of the interface. This approach not only enables the formation of a tough conformal interface between conductive polymer hydrogels and rigid electrodes, but also combines mechanical flexibility, high electrical conductivity

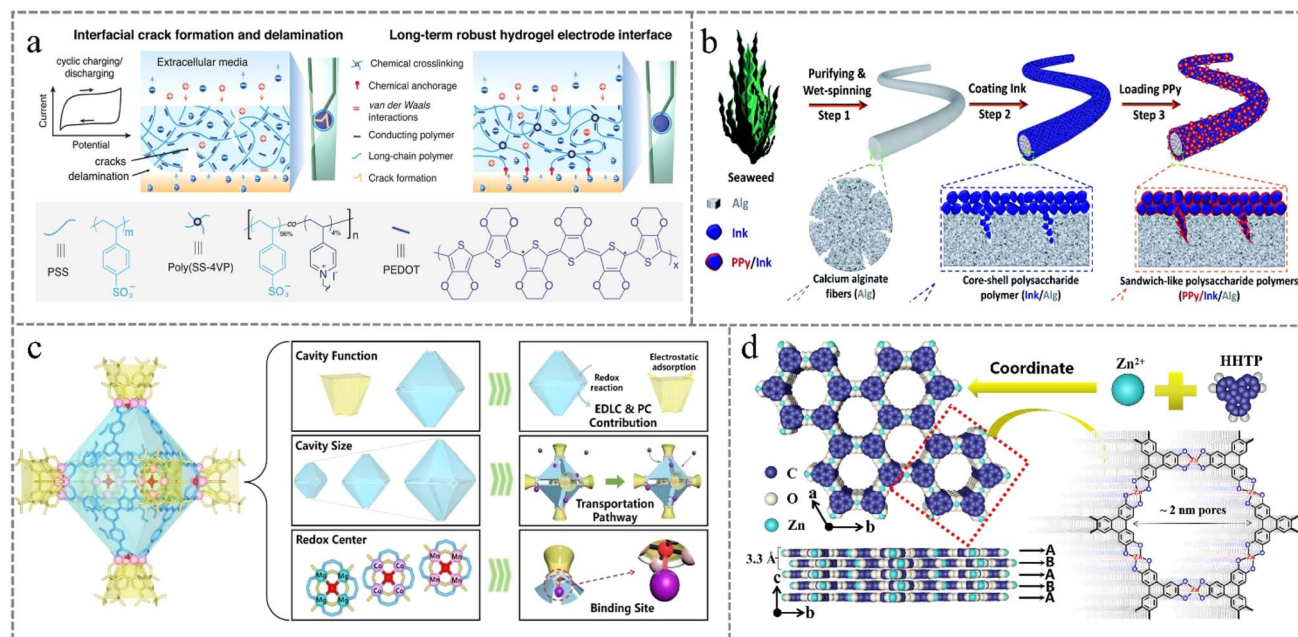


Fig. 7 (a) Conductive polymer (PEDOT) flexible electrode. Reproduced with permission from ref. 88. Copyright@2022, Wiley. (b) Algae fiber-supported conductive polymer (PPy) flexible electrode. Reproduced with permission from ref. 89. One of the authors of the article. (c) Multi-void coordination cage MOF flexible electrode. Reproduced with permission from ref. 90. Copyright@2023, American Chemical Society. (d) ZnO/Zn-MOF composite flexible electrode. Reproduced with permission from ref. 91. One of the authors of the article.

and long-term electrochemical stability. The construction strategy of such conductive hydrogel coatings provides technical support for the construction of high-performance neural interfaces and the development of next-generation brain-computer interface technologies, such as electrophysiological recording and bioelectronic therapy for neurological diseases.

PANI is a commonly used electrode material, but its structure is unstable and its cycling stability is poor when used as an electrode for energy storage devices. To optimize the structure of PANI, it is usually compounded with metal nanoparticles, conductive polymers, carbon materials, *etc.* or loaded as a functional material on the surface of flexible substrates such as fibers and fabrics. Gao *et al.*<sup>92</sup> deposited silver nanowires (AgNWs) on cotton fabrics, and AgNWs/cotton fibers were used as a conductive substrate with high electrical conductivity for charge transfer. The PANI molecular chains were then immobilized on the AgNWs/cotton fibers through a ring-opening reaction between the epoxy groups on the AgNWs/cotton fibers and the amino groups in the aniline in order to prevent them from being de-doped and to improve their cycling properties. A flexible capacitor electrode material integrating high conductivity, specific capacity and cycling performance was finally constructed. The results showed that the highest content of PANI polymerized *in situ* on the fabric surface was 20.83% when the mass ratio of aniline to modified AgNWs cotton fabric was 3 : 1. The PANI/AgNWs/cotton fiber electrode material had the highest specific capacity of 154 F g<sup>-1</sup>, which could be maintained at 96% after 5000 charge/discharge cycles. It is worth mentioning that the introduction of PANI and AgNWs can significantly improve the abrasion resistance of cotton fibers,

which increases the friction resistance of cotton fabric up to 36 000 times. Similarly, Wang *et al.*<sup>89</sup> proposed a new interfacial engineering strategy for organic–inorganic–organic composite fiber electrodes based on seaweed fibers (Fig. 7b). The seaweed fiber was soaked in ink to attach a large number of carbon nanoparticles to its surface as a conformal material to form a hierarchical core–shell structure. The PPy molecules were then deposited *in situ* on top of the alginate fibers to form a high-performance fiber-shaped electrochemical supercapacitor (FESC) layer by layer. Adequate deposition of PPy pseudocapacitor molecules on alginate fibers not only improves interfacial stability and mechanical durability, but also leads to effective electrolyte penetration and accelerated ion diffusion and transfer pathways.

**3.2.5 MOF-based electrode materials.** MOFs are an important class of porous crystalline materials constructed through coordination interactions between metal sites and organic ligands, with the inherent advantages of large specific surface area, tunable pore size, and abundant redox active sites. Among them, 2D-conducting MOFs (c-MOFs) have become a strong candidate for flexible electrode materials due to their unique structural and physicochemical properties, such as high conductivity for fast electron transport and regular nano-channels for efficient ion adsorption and desorption.<sup>93</sup> Currently, the main methods commonly used to prepare MOF flexible electrode materials include the hydrothermal method, template method, and vacuum filtration. A series of porous coordination cages (PCCs) with tunable cavities and redox metal centers were prepared and fabricated into flexible electrodes by Liu *et al.*<sup>90</sup> (Fig. 7c). The PCCs consisted of discrete metals and

organic ligands with diameters of around 1–10 nm and one or more three-dimensional cavities. PCC-11-Mn has a molecular capacitance of up to  $2510 \text{ F mmol}^{-1}$  at  $0.5 \text{ A g}^{-1}$ , a high surface capacitance of  $250 \text{ mF cm}^{-2}$  and a unique cycling stability as well as excellent capacitive properties. Unlike previously reported crystalline electrodes, PCC-11-Mn exhibits rare activation characteristics, yielding an unprecedented 115% capacitance retention after 10 000 cycles. This study provides strong theoretical support for the charge binding sites and charge transport pathways of PCC supercapacitors. Lu *et al.*<sup>94</sup> designed a simple and efficient vacuum filtration membrane fabrication technique using methylene blue (MB) as a redox indicator, and then obtained Ni-MOF composites by a calcination method, on which gold nanoparticles were deposited, and in this way, a flexible paper-based electrode based on Ni-MOF composites/gold nanoparticles/CNTs/poly(vinyl alcohol) was constructed. The interaction of MOF with single-stranded DNA (ssDNA) was realized due to the conjugated  $\pi$ -electron system of Ni-Au composites that can provide a source of hydrogen bonding. The prepared CCP membrane electrode has high sensing performance for HIV detection and can be used for the detection of target DNA in complex serum samples. The simple and inexpensive flexible paper-based MOF composite membrane electrode can also be used for the diagnosis of POC of other pathogens.

The presence of  $\pi$ -d or  $\pi$ - $\pi$  conjugation is one of the reasons that make MOFs electrically conductive, as it can endow the material with its own high electron delocalization domain, which makes electrically conductive metal-organic frameworks (EC-MOFs) widely used in electronics. The interaction mechanism between conductive 2D MOFs and flexible substrates is still unclear to meet the growing demand for next-generation wearable electronics. Wu *et al.*<sup>95</sup> synthesized conductive ultrathin Cu-BHT thin films at the liquid-liquid interface by a self-assembly method and explored the potential mechanism for the difference in conductivity on different representative substrates. The Cu-BHT/polymer layer is considered to be a friction electric nanogenerator of flexible electrodes that can harvest energy from water droplets and human motion, validating the important role of EC-MOF in flexible and wearable applications. Similarly, Liu *et al.*<sup>91</sup> constructed a layer of ZnO nano-arrays on the surface of flexible seaweed fibers by a simple low-temperature hydrothermal method and grew Zn-MOF (Zn-HHTP) on it *in situ* with sub-metal sacrificial templates (Fig. 7d). The  $\pi$ - $\pi$  conjugated structure of Zn-HHTP gives it excellent semiconducting properties, and it is directly used as an electrode for photoelectric/gas-sensitive dual-mode detection. The conductive and porous properties of Zn-HHTP make it possible to be used as either an electrode layer or as a functional layer to form a heterojunction together with ZnO for dual-mode sensing purposes.

**3.2.6 Natural macromolecules.** In addition to the aforementioned carbon-based materials, conductive polymers, MXene-based and other electrode materials, in recent years, natural macromolecular materials such as cellulose, silk protein, lignin, *etc.*, which have a porous structure, strong mechanical strength, biodegradability, and high thermal and

chemical stability, have also been used as flexible electrodes. These electrodes possess good biocompatibility as well as low host immune response.<sup>96</sup> The presence of multiple active sites on the surface accelerates re-epithelialization, wound closure, neo-angiogenesis and wound healing.

Lignin is a non-homogeneous amorphous polymer with abundant reserves on earth, and its structure is rich in hydroxyl, carboxyl, ether groups and other functional groups, the presence of which allows selective modification of this complex compound, making it a promising natural polymer. Lignin from different sources has different physicochemical properties. Industrial lignin is mainly derived from pulp and paper black liquor and biorefinery residue, and its high carbon content, high aromaticity and high calorific value are ideal carbon sources for the construction of porous carbon materials. The dignified lignin slices treated with electro-polarization can be directly used as self-supporting electrodes, which have a wide range of applications in supercapacitors and lithium-ion batteries. Liu *et al.*<sup>97</sup> prepared oriented microchannel carbon materials by carbonizing poplar delignified lignin slices. The wood delignified carbon material has a huge intertubular lumen and a uniquely aligned microchannel structure with good flexibility. This unique porous aligned microchannel structure is not only useful for greatly increasing the surface area of the electrode material accessible to the solid electrolyte, but also forms an effective and well-organized conductive pathway, which offers great possibilities for regulating the energy storage performance. Cellulose still needs to be improved in terms of conductivity, dispersion and solubility. Tanguy *et al.*<sup>98</sup> proposed a composite sensing nanopaper based on sustainable lignocellulosic nanofibers (LCNF) in the first attempt to design a high-performance and real-time gas sensor. LCNF combines reduced rGO nanosheets and PANI as the sensing layer. Due to the introduction of rGO, the sensitivity of the sensor to volatile amines was increased by a factor of 10 (*i.e.*, ammonia detection down to 1 ppm). The natural lignin on the surface of the cellulose nanofibril reduces the moisture sensitivity and provides high wet strength for the fabrication of sensors with low signal fluctuations influenced by the moisture of the surrounding environment. In addition, we demonstrate the application of sensing nanopaper in microwave sensors for battery-free, flexible and wireless applications in healthcare and environmental monitoring.

Although natural macromolecule-based flexible electrodes are ideal for use as flexible supercapacitor electrodes because of their excellent mechanical properties, high specific surface area, low density, and low coefficient of thermal expansion, improvements are still needed in terms of their conductivity, dispersion and solubility.

## 4. Manufacturing methods

Over the past few years, a large number of flexible electrodes have been fabricated through many convenient fabrication processes, such as spin-coating, layer-by-layer (LBL) assembly, vacuum filtration, *etc.* Stand-alone flexible electrodes are usually prepared by vacuum filtration, chemical vapor



deposition, and solvent heat to combine the active material with the flexible substrate to achieve integrated integration with good electrical conductivity, unique nanostructures, structural integrity, and chemical stability. However, there are drawbacks of poor mechanical properties and easy damage under continuous mechanical deformation.<sup>99,100</sup> To get a perfect flexible electronic device, it needs to have a flexible substrate, electrode layer, adhesive layer and encapsulation layer. Among them, the electrode layer, as the key to carrier transmission and signal output, is particularly important for its rational material selection and design. We discuss in detail four electrode preparation techniques (printing, vacuum filtration, deposition, and electro/chemical plating) that are currently widely used, and provide a brief introduction to others such as electrostatic spinning, solvent heating, end-base encapsulation, *etc.*

#### 4.1 Printing

The use of 3D printing technology to fabricate bioelectronic devices has attracted widespread attention because 3D printing technology shows great potential to surpass traditional manufacturing technologies in terms of versatility of materials and designs, manufacturing efficiency, process simplicity, and scalability for future mass production. The development of 3D printing technology is divided into two major directions: (i) the focus is on the large format 3D printing technology; (ii) the focus is on the microscopic aspect of printing technology. The second method is more precise and detailed, and is often used to manufacture flexible electrodes with flexibility, portability and integration of minuteness.<sup>101,102</sup> Commonly used processes include direct ink writing (DIW), electric field driven (EFD) processes, fused deposition molding (FDM), stereolithography (SLA), material jetting (M-Jet), binder jetting, directed energy deposition (DED), and sheet lamination.

Zhao *et al.*<sup>103</sup> selected PI as the substrate layer, stretchable silver paste as the conductive layer, and Ecoflex 0030 silica gel as the encapsulation layer (Fig. 8a). A high-density electrode array with a 32-channel multilayer stacked thin film structure, including a planar substrate layer, a  $4 \times 8$  arrayed circular electrode conductive layer, a porous flexible encapsulation layer, and a micro-convex electrode filler layer, was prepared based on a DIW 3D printer mechanism. The integrated and customized fabrication of flexible high-density EMG electrode arrays was achieved. It is experimentally found that the array electrodes can accurately detect the spatiotemporal characteristics of muscle activation, which can ensure the inverse solution of a credible motor unit discharge sequence, and is expected to be applied to the field of human-machine interfaces based on the inverse solution of high-density surface EMG. Zhu *et al.*<sup>104</sup> present a mask-less, template-less, and plating-less fabrication technique for embedded silver mesh flexible transparent electrodes (FTEs) by combining electric field-driven (EFD) micro-3D printing technology with a newly developed hybrid hot pressing process (Fig. 8b). A high-resolution and high-AR silver mesh is fabricated using the EFD micro-3D printing process, and then embedded in a thermoplastic flexible transparent substrate using a roll-assisted hybrid hot

pressing process to obtain the final FTE. The FTE fabricated by the method is highly transparent, has strong adhesion, stable performance, and corrosion-resistance, and exhibits a high scratch-resistance with a hardness of 3H. The method is based on the use of the EFD micro-3D printing process and the newly developed EFD micro-3D printing process to fabricate FTE. The method eliminates the conventional photomask, vacuum deposition, stencil, and electroplating processes to produce high-performance FTEs with embedded silver mesh, and produces FTEs with controllable thickness and excellent surface roughness ( $R_a \approx 18.8$  nm) without any polishing treatment. Microelectrode arrays provide a way to record electrophysiological activity critical to brain research. However, there are still drawbacks: (i) the inability to customize the electrode layout to meet specific experimental or clinical needs, and (ii) the significant limitations of current electrodes in terms of coverage, vulnerability, and cost. Based on this, Saleh *et al.*<sup>108</sup> demonstrated a rapid 3D additive printing method for creating CMU arrays and showed its operation for penetrating and recording biological tissues. This fabrication method also allows for flexible reconfiguration, including different individual shank lengths and layouts, with low overall channel impedance. This technique paves the way for customizable large-scale probes (thousands of channels over an area of a few square centimeters) with easy-to-modify probe layouts that can capture and potentially manipulate the dynamics of large multiregional neural circuits with single neuron and single millisecond resolution.

Transfer printing is another effective method for realizing high-performance 3D electronics.<sup>99,100</sup> Chen *et al.*<sup>105</sup> proposed a wrap-like transfer printing strategy for fabricating 3D curved electronics relying on homemade prototypes (Fig. 8c). Pre-fabricated planar circuits on a petal-like impression are completely integrated onto and fully cover the target surface with the assistance of a mild and uniform pressure field. The driving pressure for winding is provided by strain recovery of a pre-strained elastic film triggered by pneumatic pressure control. Guided by the results of finite element analysis, the wrap-around transfer printing strategy is optimized in terms of the number of petals, the thickness of the impression and the pre-cutting treatment. The method was applied to different curved surfaces, including sphere, ellipsoid, and cornea shapes, and showed good consistency of the electronics, tabulating its feasibility in the development of complex 3D curved electronics. Conventional printing methods are unable to utilize designed micropatterns for mechanical deformation and multilayer integration, restricting the deployable functionality of the electrodes. Ershad *et al.*<sup>106</sup> reported a high-density myoelectric mapping with a customizable and reconfigurable on-skin drawn MEA (DoS MEA) (Fig. 8d). The high-density DoS MEA was fabricated in minutes with biocompatible conductive inks based on Ag-PEDOT:PSS composites, water/acrylic emulsion-based insulators, ballpoint pens, and stencils. Compared to current wearable bioelectronic devices, the DoS MEA shows minimal variability in its electrical properties, despite the hand-performed drawing process by the human user. Sutherland *et al.* developed a compatible strategy for high-throughput roll-

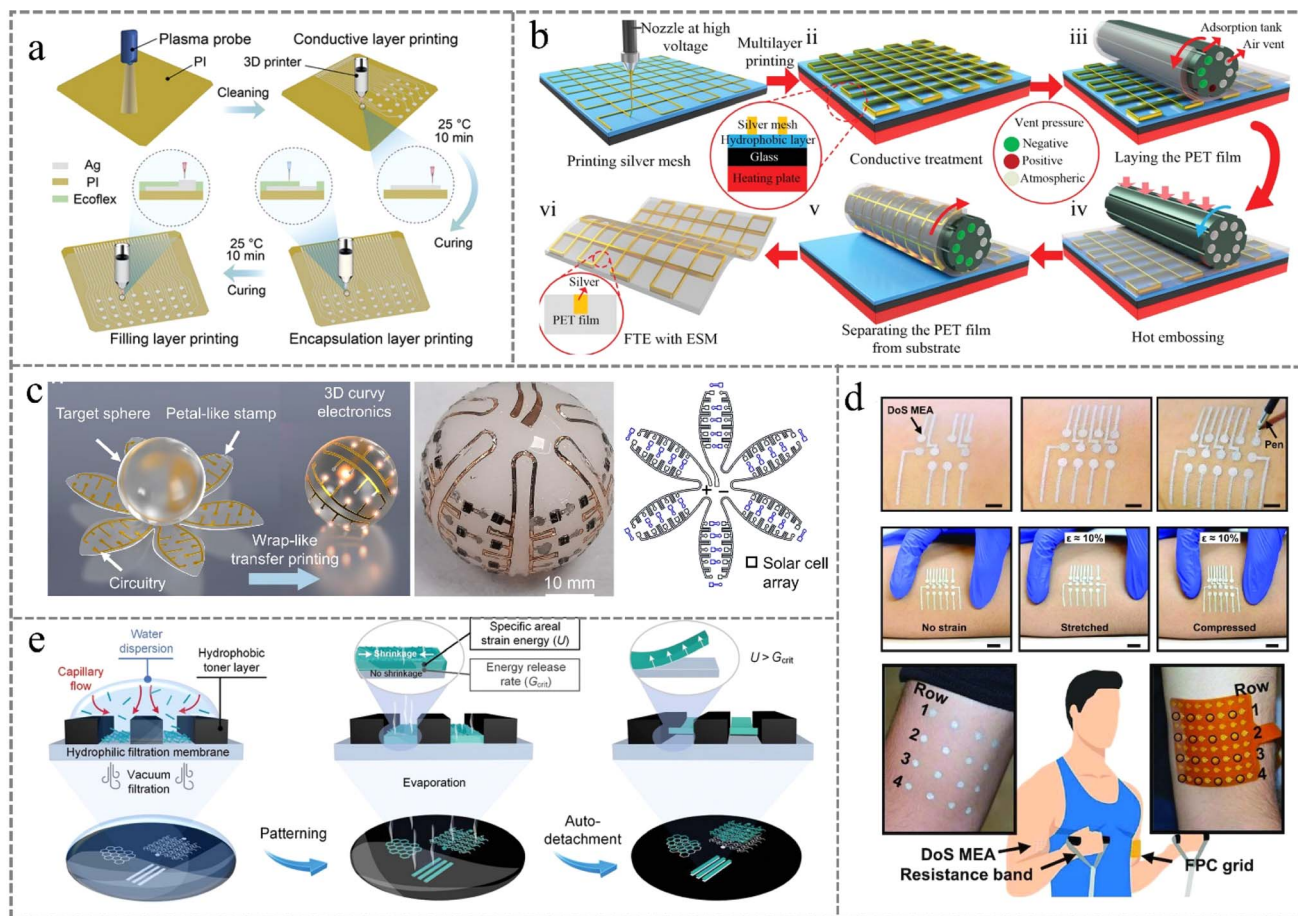


Fig. 8 (a) 3D printed high-density flexible electrode. Reproduced with permission from ref. 103. Copyright@2023, Wiley. (b) 3D printed flexible transparent electrode. Reproduced with permission from ref. 104. Copyright@2021, Wiley. (c) Wrap-around transfer printed electrode. Reproduced with permission from ref. 105. Copyright@2023, American Association for the Advancement of Science. (d) Customizable and reconfigurable direct-write printed electrodes. Reproduced with permission from ref. 106. Copyright@2022, Oxford University Press. (e) Automatically removable patterned electrodes produced by vacuum filtration. Reproduced with permission from ref. 107. Copyright@2022, Wiley.

to-roll (R2R) preparation of electrodes for flexible chalcogenide solar cells (PSCs) under laboratory environmental conditions.<sup>109</sup> The silver (Ag)/carbon electrodes were prepared on flexible substrates by a printing technique, which were then transferred to a printed PSC precursor stack by a dry pressure deposition (DPD) method. This method avoids the potential loss of PSC performance due to solvent migration of the paste, which in turn improves the performance and stability of the PSCs.

#### 4.2 Vacuum filtration

Compared with other methods, vacuum filtration is characterized by simplicity, speed, low cost and wide applicability of materials. Moreover, high-density flexible electrodes can be obtained by vacuum pressure control and combined with cold or hot pressing at a later stage. In addition, some non-conductive groups (*e.g.* PSS in PEDOT:PSS) can be removed during the filtration process to further enhance the material properties. Therefore, the vacuum filtration process has been widely adopted to prepare flexible electronic devices. A flexible but robust  $\text{Ti}_3\text{C}_2\text{Tx}$  MXene/bamboo microfiber (BF) composite

paper was reported by Zhu *et al.*<sup>110</sup> through a simple vacuum filtration process. Due to the excellent compatibility between MXene and BF, the MXene/BF composite paper exhibited both excellent tensile strength of 49.5 MPa, higher than that of the MXene sheet and BF film alone, and excellent electrical stability with no detectable degradation after 1000 tensile, bending, and compression cycles. More importantly, the electrical conductivity of MXene/BF composite paper is highly stabilized during bending, stretching and compression, thus making MXene/BF composites excellent conductors.

Masked vacuum filtration is a fast, high-throughput, and scalable method for the preparation of thin film electrodes. Lv *et al.*<sup>107</sup> invented an evaporation shrinkage-assisted patterning (SHAPE) method to fabricate auto-removable, freestanding, and patternable electrodes by employing evaporation-induced interfacial strain mismatches (Fig. 8e). The SHAPE method utilizes vacuum filtration of PANI/bacterial cellulose (PANI/BC) ink through a masked filter membrane to print high-resolution, patterned and multilayered electrodes. Strong interlayer hydrogen bonding ensures strong multilayer membrane

integrity, while the controlled evaporation shrinkage properties of PANI/BC lead to a mismatch between the electrode strain and the interfacial filtration membrane, resulting in automatic electrode separation. The 500-layer substrate-less micro-supercapacitor fabricated by this method has an energy density of  $350 \text{ mW h cm}^{-2}$  and a power density of  $40 \text{ mW cm}^{-2}$ , which is 100 times higher than those of the reported substrate-limited counterparts. Jiang *et al.*<sup>111</sup> introduced antimonene (Sb) nanosheets with ultrathin thickness, excellent mechanical strength and flexibility into PANI electrodeposited CNT frameworks by a simple vacuum filtration strategy to achieve continuous and uniform growth of PANI. A freestanding Sb/CNT/PANI electrode was successfully fabricated, and the simple strategy reported in this paper provides ideas for the design of high-performance flexible electrode materials to meet the demands of portable and wearable electronics. The self-supported films prepared by vacuum filtration are currently limited to micrometer thickness, and the preparation and transfer of nanometer-thick films will further broaden the application of this process if it can be realized in the future.

### 4.3 Deposition

The method mainly includes physical deposition, chemical vapor deposition and electrochemical deposition. It is a more efficient and accurate method in the preparation of flexible electrodes. Lyu *et al.*<sup>112</sup> deposited a 50 nm thick cPVP layer on a PEN substrate, and the hydrophobic cPVP surface was transformed into a hydrophilic surface by UV/ozone treatment

(Fig. 9a). The MXene electrodes were then large-scale patterned using a selective wetting method, and then a 500 nm thick cPVP gate dielectric layer was rotationally coated onto the substrate containing the MXene gate electrode pattern. Large-scale, homogeneous MXene electrode arrays were prepared and used for high-performance OFETs. The operating capability of the MXene electrodes was effectively tuned by  $\text{NH}_3$  chemical doping. In addition, complementary circuits such as NOT, NAND, and NOR were fabricated by integrating p-type and n-type OFETs.

Chemical deposition is an efficient and precise method for the preparation of membrane electrodes, and is generally carried out in a three-electrode plating bath, where catalyst particles are uniformly deposited onto a proton exchange membrane or a gas diffusion layer under the action of an applied electric field to complete the preparation of membrane electrodes. Gou *et al.*<sup>117</sup> have innovated a nickel-foam-catalyzed chemical deposition (NFED) method for the preparation of 3D metal-patterned embroidered electrodes, which was first applied in the battery field. The nickel foam can initiate and catalyze the chemical deposition reaction, which has a role similar to that of an antitemplate in the field of screen printing, and the method is controllable and economically feasible. Modeled on Li-S and Li-LiFePO<sub>4</sub> batteries, the embroidered electrodes maintain excellent electrochemical performance under high deformation. This provides a new idea for the development of next-generation flexible energy storage devices. Kafle *et al.*<sup>113</sup> used carbon cloth as a flexible substrate and

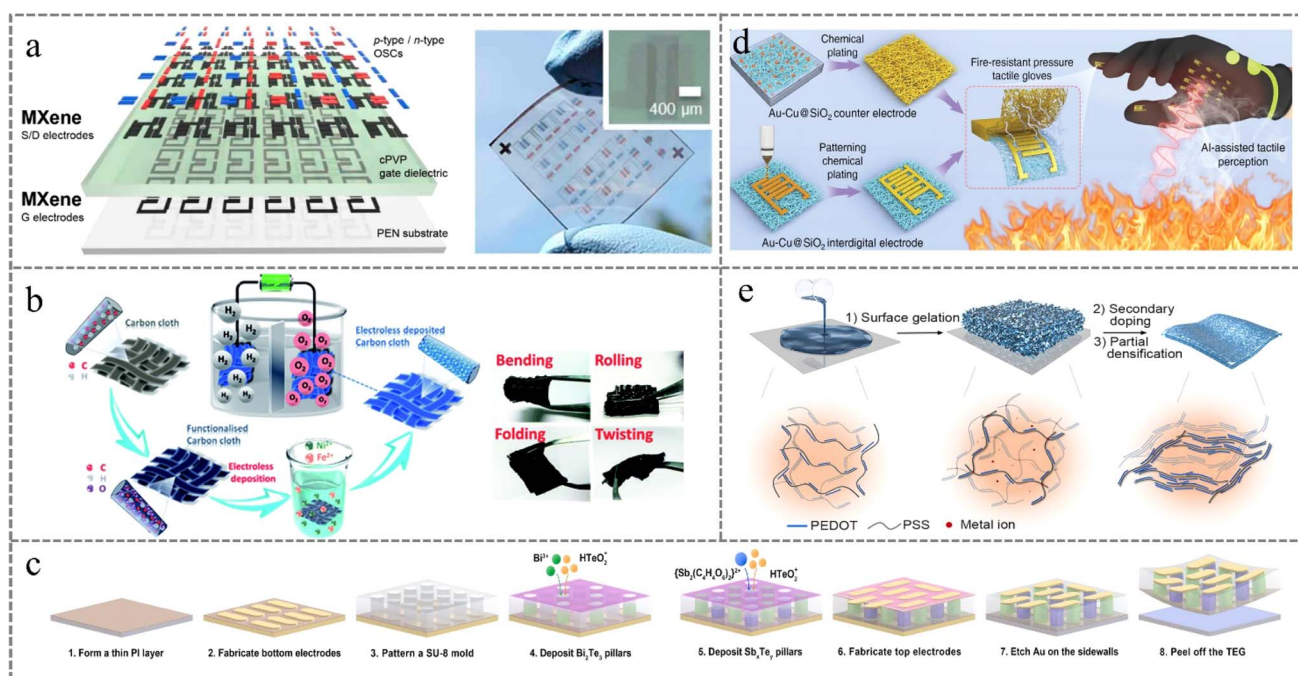


Fig. 9 (a) Deposition method for the preparation of large area MXene electrode arrays. Reproduced with permission from ref. 112. Copyright©2019, American Chemical Society. (b) Activation-free chemical deposition of NiFe on carbon cloth as a self-supporting flexible electrode. Reproduced with permission from ref. 113. Copyright©2021, Royal Society of Chemistry. (c) Ultra-light weight flexible electrode by an electroplating method. Reproduced with permission from ref. 114. Copyright©2023, Elsevier. (d) Large-scale synthesis of refractory electrodes by electroplating. Reproduced with permission from ref. 115. Copyright©2024, Wiley. (e) Suspension cross-linking technique for the preparation of hydrogel/conducting polymer composite electrodes. Reproduced with permission from ref. 116. This is an open access article.



deposited NiFeS and NiFeP on carbon cloth by a single-step chemical deposition method, which was used to prepare simple and economical self-supporting flexible electrodes, improving the sensitization and activation steps in the conventional process (Fig. 9b). NiFeS@OCC and NiFeP@OCC have excellent OER activity and stability, reaching 10 mA cm<sup>2</sup> at overpotentials of 220 and 270 mV, respectively. The anti-deformation stability as well as efficient electrocatalytic activity of these two electrode materials proved that they can be used as OER catalysts, which provides a new direction for the development of flexible devices that are simple to prepare and work efficiently.

#### 4.4 Electro/chemical plating

Zhang *et al.*<sup>114</sup> reported the preparation of flexible micro thermoelectric generators (TEGs) with high power density and light weight by utilizing pulse plating technology, as well as micro-nano-machining and stripping techniques (Fig. 9c). The optimized preparation process resulted in TEGs with high flexibility and an ultra-light weight of 0.0246 g. The TEGs were fabricated with a high power density and ultra-light weight. The weight ratio and thermoelectric properties can be effectively controlled by adjusting the plating process. By reducing the electrical contact resistance through the deposition–dissolution treatment, the voltage factor and normalized power-to-weight ratio of the TEG are more than three times higher than those of the cross-plane flexible TEGs in the literature, and the power generation performance of the electroplated flexible micro-TEGs is dramatically improved, demonstrating its potential as a miniaturized power source for wearable electronics.

Ceramics are commonly used as substrate materials in rigid electronic devices, but the instability of their performance under high temperature and large deformation conditions is one of the reasons hindering their development. Enhancing the interlayer bonding through flexible ceramics is particularly important. Gao *et al.*<sup>115</sup> firstly prepared a large flexible SiO<sub>2</sub> nanofiber (NF) film by electrostatic spinning, and then deposited a Cu/Au nanolayer on it by chemical plating to form a sensitive inter-digital electrode sensor, and then used an *in situ* thermal reaction strategy to form a co-conformally interlocked Au<sub>3</sub>Cu and CuSiO<sub>3</sub> interface (Fig. 9d). With the sensing electrode layer prepared by this method, the stiffness matching and strong combination at the contact enhanced the mechanical–thermal stability of the electrodes, enabling the stable application of this sensor in the field of fire-resistant pressure tactile sensing. Pan *et al.*<sup>118</sup> fabricated polymer microneedle arrays on flexible substrates by optical 3D microprinting. Then, gold-plated interdigital electrodes were prepared using a light-assisted chemical plating process. A novel hybrid device of microneedle arrays and interdigital electrodes was assembled on this basis for electrical stimulation-mediated antitumor immunomodulation. This flexible microneedle array integrated interdigital electrode (FMIE), which is simple to prepare, and gold-plated polymer microneedles with precise geometries and dimensions can be fabricated simultaneously with a flexible gold-based interdigital electrode, has some potential for clinical

translation and application. Hao *et al.*<sup>119</sup> used hydrophilic flexible filter paper as a flexible substrate on which nickel sulfide was modified using carbon quantum dots (CDs) by a mild chemical plating method to prepare highly efficient and stable industrial grade catalytic electrodes with high current density (CDs-Ni<sub>3</sub>S<sub>2</sub>@NFP). The unique CDs-Ni<sub>3</sub>S<sub>2</sub>@NFP electrode can efficiently prepare sulfur-based catalytic materials with large surface area and high catalytic activity at room temperature. This work provides technical support for the efficient catalysis of flexible catalytic electrodes for water cracking, energy storage, and device preparation.

#### 4.5 Others

Technologies such as printing, vacuum filtration, deposition, electro/chemical plating *etc.*, as mentioned above, are mainly for composite electrodes based on nanoactive materials. However, many conductive fibers/fabrics, stretchable hydrogels/aerogels, and conductive polymer films can be used as stand-alone flexible electrode materials and directly integrated into flexible electronic devices. This involves several other methods, such as electrostatic spinning, solvent heating, end-base encapsulation, *etc.* The design and preparation of free-standing flexible electrodes will be uniformly discussed here.

Yao *et al.*<sup>116</sup> synthesized PEDOT:PSS-based conductive polymer (CP) hydrogel films by crosslinking a commercial CP suspension onto a PDMS substrate coated with iron carbonyl particles (Femp) (Fig. 9e). The surface gels were combined with secondary doping and partial densification to fabricate CP hydrogels with such desirable complex nanostructures. Based on PEDOT:PSS as the exemplary model material in this work, such CP hydrogels have superb, high conductivity and capacitance. This strategy significantly reduces the low-frequency impedance and improves the signal fidelity without compromising its high-frequency response. In addition, excellent biocompatibility and multifunctionality are demonstrated, showing the great potential of this strategy for bioelectronic applications and human–machine interfaces. Highly sensitive flexible pressure sensors with a wide range of pressure responses are highly needed in tactile recognition applications. Li *et al.*<sup>120</sup> prepared a breathable polycaprolactone nanofiber substrate by an electrostatic spinning process, and three layers of conductive nanofiber membranes with different resistances as sensing layers of sensors by a simple process of *in situ* polymerization of aniline and spraying of silver nanowires. Meanwhile, a copper nanowire network was prepared as the sensor electrode by wet oxidation and electrochemical reduction to ensure the permeability and stability of the device. The sensor was further integrated into a 5 × 5 array system. It can accurately respond to the spatial position distribution of an object and is applied to simulate sitting posture monitoring.

Implantable electrodes are used in the biomedical field to monitor and transmit electrical impulse signals in the body, and often require human tissue attachment. However, most human organ tissues are soft and fragile, and the rigid electrode materials used in existing devices do not match the viscoelastic biological tissues for a perfect fit, and the applied stresses tend

to cause permanent deformation of the organs. A viscoelastic surface microelectrode array was reported by Tringides *et al.*<sup>121</sup> The prepared sodium alginate hydrogel was cross-linked by ions and was not insulating itself, thus requiring the addition of a viscoelastic encapsulation layer on the surface. The amino-capsule technique was utilized to enhance the force between the two, stretching to 10 times its own length without breaking. This work replaces the traditional rigid conductive elements and encapsulation techniques, and the sensors can be tightly fitted to the body's organs, receiving and transmitting electrical impulse signals to minimize the risk of damage to fragile organs.

Wang *et al.*<sup>122</sup> synthesized an efficient CO gas sensor based on a ZnO/SnSe<sub>2</sub> composite film using simple hydrothermal and template sacrificial methods. The ZnO/SnSe<sub>2</sub> composite sensor has good selectivity and dynamic characteristics for CO at room temperature. And it was verified that the UV light could improve the gas-sensitive characteristics of the sensor. The possible CO sensing mechanism is related to the heterogeneous structure between n-type SnSe<sub>2</sub> and n-type ZnO nanomaterials and the photoelectrons excited by UV light. Li *et al.*<sup>123</sup> prepared flexible photodetectors by solution-processed micrometer-scale Cu electrodes and high-quality InSe nanosheets. For the first time, lithography was successfully integrated with PAMD to fabricate flexible Cu electrodes with micrometer resolution and high throughput on a thin polymer substrate, which provides an effective solution for the high-volume preparation of metal electrodes on large-scale flexible substrates.

## 5. Applications

### 5.1 Flexible sensors

**5.1.1 Pressure sensor.** Flexible pressure sensors are an important component of flexible electronic devices. And flexible pressure sensors have a wide range of applications due to their excellent mechanical and electrical properties, such as high flexibility, high sensitivity, high resolution and fast response.<sup>124,125</sup> According to the working mechanism of pressure sensors, they can be broadly classified into the following categories: piezoresistive, capacitive, piezoelectric and other types of pressure sensors. In the past decade, research on flexible wearable sensor devices has grown rapidly, and with the booming development of intelligent robots and wearable electronic devices, research on various new devices based on flexible pressure sensors that conform to arbitrarily curved surfaces is also proceeding rapidly, and flexible sensing technology will play an increasingly important role in the future.<sup>35,126,127</sup>

Du *et al.*<sup>128</sup> have successfully developed a lightweight, breathable, biocompatible and highly sensitive flexible piezoresistive pressure sensor based on an all-fiber structure and a PI insulating layer by continuous optimization of both sensor structure design and material selection (Fig. 10a). The sensor possesses a high sensitivity of 1970.65 kPa<sup>-1</sup>, which is approximately 13 times higher than that of the sensor without the insulating layer. And it exhibits excellent cycling stability of more than 10 000 cycles and a fast response/recovery time of 10/20 ms. In addition, the sensor is capable of sensing human

motion, from small movements (*e.g.*, pulse) to large movements (*e.g.*, knee bends). These superior properties provide a good foundation for applications in comprehensive human motion monitoring and pressure spatial distribution detection. This study provides an effective strategy for fabricating flexible pressure sensors with good overall performance in the field of smart wearable electronics. Li *et al.*<sup>133</sup> prepared and obtained efficient flexible tactile sensors for human motion monitoring and recognition by an electrostatic spinning technique. The sensor is made of a PVDF-based nanofiber (NF) membrane, which is low-cost and easy to assemble. The PVDF-based ESNF membrane has good mechanical and electrical properties, making the sensor self-powered, lightweight, breathable, and robust. The assembled PENG sensing device has excellent sensitivity over a wide pressure range, a fast response time of 82.7 ms, and excellent durability over 12 000 loading test cycles. Gao *et al.*<sup>134</sup> developed an all-paper-based piezoresistive (APBP) single-use pressure sensor through a simple, economical, and environmentally friendly method. The sensor uses thin paper with a porous structure and rough surface as a flexible substrate and silver nanowires (AgNWs) as a sensing layer. Nanocellulose paper (NCP) was used as the bottom substrate and top encapsulation layer for the printed electrodes. The APBP pressure sensor was tested to have a high sensitivity of 1.5 kPa<sup>-1</sup> in the range of 0.03–30.2 kPa and excellent bending resistance. The method is simple, low-cost and environmentally friendly, and is expected to promote the development of single-use pressure sensors and green paper-based flexible electronic devices. Graphene is a common flexible electrode material, but it is still limited in practical applications by sensor array structural mismatch, integration bias, *etc.* Kim *et al.*<sup>135</sup> designed a skin-fitting flexible pressure sensor array by utilizing graphene nanoplatelets (GNP) as the active material. An electrical circuit method was proposed, which employs cubic spline interpolation to achieve a wide range of calibration for the sensor array operation. The calibrated response of a flexible sensor array attached to a human arm with inhomogeneous surface curvature was successfully obtained. This work opens the way for flexible pressure sensor arrays attached to the skin to provide reliable resistive responses under different external pressures and is a practical approach to various sensor technology ideas.

**5.1.2 Electrochemical sensors.** Wearable sweat detection devices have the significance of determining the human health status more directly and accurately. Therefore, research on wearable sweat sensors is one of the focuses of the current development in the field of wearable electronic health devices.<sup>136,137</sup> Zhao *et al.*<sup>138</sup> designed an integrated thread-based wearable electrochemical sensor for accurate detection of lactic acid and sodium in human sweat during exercise. The sensor was constructed using the low-temperature hydrothermal method on threaded carbon electrodes with ZnO NWs as the sensing electrodes, and two thread-based electrochemical cells were used for attachment to the skin, which generates an electrical signal when the user's perspiration is transported to the sensors while sweating. The linear ranges for lactate and sodium ions in sweat were 0–25 mM and 0.1–100 mM, respectively, and the detection limits were 3.61 mM and 0.16 mM,

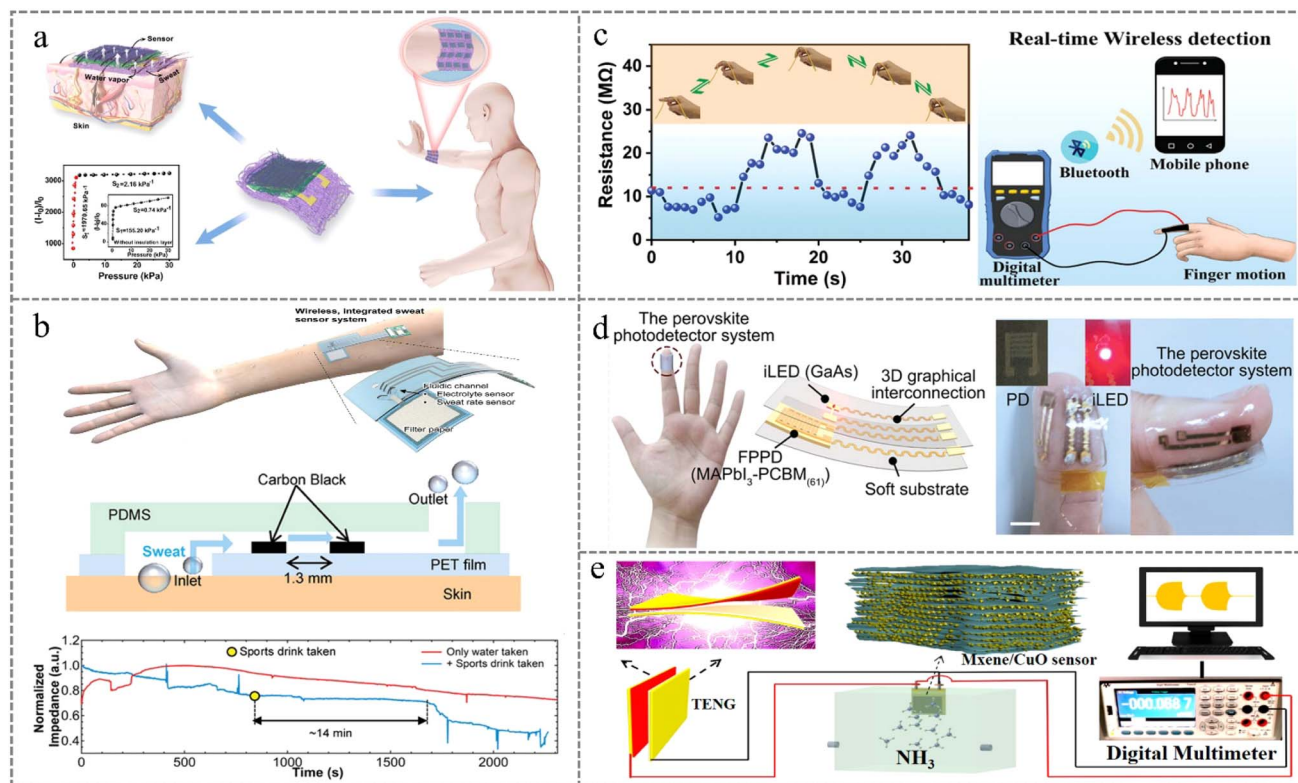


Fig. 10 (a) All-fiber piezoresistive sensor for human physiological motion monitoring. Reproduced with permission from ref. 128. Copyright©2022, Elsevier. (b) Wireless, flexible sweat rate sensor system for early, real-time dehydration detection. Reproduced with permission from ref. 129. Copyright©2023, Wiley. (c) High-performance, wearable multifunctional human motion and skin temperature detection sensor. Reproduced with permission from ref. 130. Copyright©2022, Wiley. (d) Optoelectronic integrated system for real-time monitoring of cardiovascular physiological signals and limb health. Reproduced with permission from ref. 131. Copyright©2023, Wiley. (e) CuO nanohybrid ammonia sensor for self-powered organoid MXene/metal-organic framework derivation. Reproduced with permission from ref. 132. Copyright©2021, American Chemical Society.

respectively. This electrochemical sensor can find practical applications in monitoring physiological status during human fitness for the purpose of real-time monitoring of physiological conductance and detection of electrolyte imbalance.

Electrochemical sensing based on conventional rigid electrodes has significant limitations for characterizing deformed cells or biomolecules in soft tissues. The recent emergence of flexible stretchable sensors allows electrodes to be in conformal contact with curved surfaces and to conform perfectly to the deformation of living cells and tissues. This provides a powerful strategy for real-time monitoring of biomolecules from mechanically deformed cells, tissues, and organisms, and opens up new opportunities for exploring mechano-transduction processes. Tu *et al.*<sup>139</sup> reported a wireless wearable biosensor (InflaStat) for real-time electrochemical detection of the inflammatory biomarker C-reactive protein (CRP) in sweat. The device consists of an autonomous iontophoresis module that integrates ion introduction for sweat extraction, micro-fluidic channels for sweat sampling and reagent delivery and replacement, and a graphene-based sensor array. The integrated graphene sensors for measuring pH, temperature, and ionic strength enable real-time, personalized CRP data calibration to mitigate sensing errors caused by changes in the

matrix of the interpersonal samples and to provide a more comprehensive assessment of the inflammatory status. This demonstrates the utility of this technology for non-invasive disease classification, monitoring and management. Honda *et al.*<sup>129</sup> present a wireless integrated ionic and sweat rate sensor piece for dehydration monitoring that is wireless, wearable, and easy to integrate (Fig. 10b). By developing a new sensor structure, the ionic composition and perspiration rate can be monitored simultaneously for a long period of time. Machine learning algorithms are combined to accurately predict the device tilt angle to calibrate the sensor output signal. By developing an integrated sensor system and optimizing the device structure, continuous monitoring of large total sweat volume corresponding to long-term measurements was achieved. The large volume sweat rate was continuously monitored for more than 7000 s (total sweat volume >170  $\mu$ L). Physiological responses to sports drink ingestion were confirmed by measuring changes in sweating rhythms in real time, continuous sweating impedance and rate extraction, tested on 10 subjects. Although this research is still in its preliminary stages, the system is a good platform to demonstrate the benefits of flexible medical electronics.



Ning *et al.*<sup>140</sup> developed an efficient and portable sweat sensing system that is wireless, battery-free, flexible, and self-pumping for real-time monitoring of levodopa and vitamin C levels in human sweat. The sensitivities of the sensors for levodopa and vitamin C were 0.0073 and 0.0018  $\mu\text{A } \mu\text{M}^{-1}$ , respectively, and the detection correlation coefficients were both greater than 0.99. The linear detection ranges were 0–100  $\mu\text{M}$  and 0–1000  $\mu\text{M}$ , respectively. The flexible wireless circuit boards were equipped with wireless charging, electrical signal capture and processing, and wireless transmission functions. The data recorded by each sensor was displayed on a smartphone through a self-developed application. The experimental results confirm the reliability of the sweat sensing system for non-invasive monitoring of important biomarkers in the human body and its potential use in comprehensive biological health assessment. Li *et al.*<sup>141</sup> reported a finger-based wearable sensing system (FGE) for rapid on-site detection of marker substances in animal-derived foods such as pork and milk. The sensor can be ready in tens of minutes as the laser allows rapid preparation of the FGE. Subsequently, it is connected to a portable instrument. The wearable system enables direct detection of flat surfaces (*e.g.* glass) and liquid objects on the surface of pork by direct finger contact, and of solid powders by curing a hydrogel on the electrode surface.

**5.1.3 Human motion tracking sensors.** Flexible fabric sensors, which are soft, moisture-absorbent and breathable, inexpensive, and easier to integrate with garments, have greatly improved the comfort of smart garments. In the case of motion monitoring, the detection and conversion of physiological responses to electrical signals under prolonged and dynamic measurement conditions is essential for the operation of health monitoring systems and human–computer interaction devices. An important challenge in tracking these bioelectrical signals is the availability of electrodes with high tracking quality and patient comfort. Due to the high amount of sweating during training and the exposure to light during outdoor training, higher demands are placed on the light and sweat resistance of fabrics.<sup>136,137,142,143</sup> Meanwhile, smart electronic devices in the form of wearable smart fabrics, e-skin, body domain nets and bioelectronic masks have been widely studied to realize motion tracking, gesture recognition, physiological state monitoring and human–computer interaction.

A sedentary lifestyle is listed by the World Health Organization as one of the ten major causes of death and disease. A prolonged sedentary state of the human body will reduce energy consumption and slow down blood flow, which may lead to various kinds of physical diseases in the long run. Therefore, it is important to provide timely monitoring and feedback on human sitting posture and movement status, and Ma *et al.*<sup>144</sup> developed a non-contact sitting posture and movement status tracking and vital signs detection technology by using a cross-linked polypropylene (IXPP) piezoelectric electret film (piezoelectric sensing layer) and a plain conductive fabric tape (electrode layer) to design and prepare a flexible piezoelectric thin-film sensor. The core component of the technology is a highly sensitive flexible pressure sensor based on a new artificial microstructured smart material, the piezoelectric electret film.

The sensor can be embedded in the cushion/seat to realize the real-time, non-sensory monitoring of the human body's sitting posture and motion status tracking and vital signs signals. The sensor structure is designed with a folding process, which can enhance the output signal to double that of a single layer without changing the sensing area, and has a higher signal-to-noise ratio, which can meet the requirements for real-time and accurate monitoring of large or weak human motion signals. Inspired by embroidery technology, Zhao *et al.*<sup>145</sup> proposed a fully woven 3D fabric electrode, which selects water-retaining and conductive composite yarn as the flexible electrode substrate, and reduces graphene oxide (RGO) and silk glue as the coating material. The water-retaining ability of the yarn itself as well as the fluffy structure can form good contact with the skin, enhance the electrode contact and improve the quality of the signal, which can be used for both long-term and motion state monitoring applications. The porous structure of knitted electrodes further provides the user comfort due to their soft touch formation and breathability. Electromyography (EMG) and electrocardiography (ECG) signals have been analyzed experimentally and definitively. Lin *et al.*<sup>130</sup> reported the rational design of a multifunctional flexible sensor material with high sensitivity, low detection limit, high-temperature coefficient, and high mechanical strength based on carboxystyrene butadiene rubber (XSBR) and hydrophilic silk rubber (SS) noncovalent bond-modified CNTs into a multifunctional sensor (Fig. 10c). The rubber-based sensor has an integrated tracking capability of real-time, *in situ* physiological signals to detect weak and large deformations, with a lower detection limit of 1% strain, an elongation of up to 217%, a strength of 12.58 MPa, a high sensitivity, a measurement coefficient of up to 25.98, a conductivity of 0.071  $\text{S m}^{-1}$ , and a percolation threshold of 0.504 wt%. This provides a new way to develop wearable artificial intelligence in human health and motion monitoring.

**5.1.4 Photoelectric sensors.** The application of most flexible materials in optoelectronics as electrodes is limited by the trade-off between high transmittance and low conductive resistance, as low resistance requires more conductive material, which reduces light transmission by generating greater surface coverage. Flexible photodetectors (FPDs) with excellent optoelectronic properties and mechanical flexibility have attracted great interest in a variety of applications, including wearable health monitoring, implantable optoelectronics, and artificial vision systems.<sup>146,147</sup> Tang *et al.*<sup>148</sup> proposed an electric field modulation strategy to significantly reduce the dark current of metal halide chalcogenide-based flexible photodetectors by more than 1000 times (from  $\sim 5$  nA to  $\sim 5$  pA). Moreover, the strategy effectively suppresses ion migration in metal halide chalcogenides, and the metal halide chalcogenide-based flexible photodetectors show long-term continuous operational stability ( $\sim 8000$  s) with low signal drift ( $\sim 4.2 \times 10^{-4}$  pA per second) and ultra-low dark current drift ( $\sim 1.3 \times 10^{-4}$  pA per second). Thanks to the electrical modulation strategy, a wearable photovoltaic volume tracing sensor with a high signal-to-noise ratio and an active matrix photodetector array for low-light imaging was successfully demonstrated. A general

strategy is provided to improve the performance of metal halide chalcogenides for wearable flexible photodetector and image sensor applications.

Photoelectric volumetric pulse wave (PPG) is a typical sensing method in the field of photoelectric sensing that is technologically advanced, stable and easy to operate. However, the human body is in a constant state of motion, resulting in unstable device signal acquisition, especially skin and joints, both of which have a certain degree of intrinsic ductility and significant mobility. An effective solution is to transfer printed or fabricated photovoltaic devices onto flexible substrates. Wu *et al.*<sup>131</sup> demonstrated a patch-type photovoltaic system that integrates flexible chalcogenide photodetectors and fully inorganic light-emitting diodes to enable real-time monitoring of human PPG signals (Fig. 10d). Using the photodetector, human pulse rate and swelling of finger joints can be extracted and analyzed to monitor human health for prevention and early diagnosis of certain diseases. A 3D pleated serpentine interconnect was developed to improve the shape adaptability of the device for practical applications. A new type of flexible organic phototransistor (OPT) was prepared by Zhong *et al.*<sup>149</sup> The ultrashort channel length based on bulk heterojunction (BHJ) mixtures has an airfield effect, which enables the OPTs to have excellent photoresponsiveness, detectability, and flexibility. Due to the nanoscale channel length and BHJ structure, photoexcitons can be efficiently separated into free carriers and rapidly transferred vertically to the electrodes. The sensor response is up to  $750 \text{ A W}^{-1}$ , and the detectivity and photo-sensitivity are  $4.54 \times 10^{15}$  jones and  $1 \times 10^6$ , respectively, which are superior to conventional transverse organic phototransistors under light illumination. Based on the rational structural design and semiconductor morphology monitoring, the phototransistor has great potential for application in flexible organic electronics.

The development of an efficient fabrication process for high-resolution chalcogenide pixel arrays is key to the realization of large-scale flexible image sensors. Wang *et al.*<sup>150</sup> demonstrated an improved sequential deposition approach to fabricate large-scale quasi-two-dimensional thin-film arrays for optical sensing and imaging with precise pixel locations and controllable morphology. The crystallinity of the chalcogenide films was improved by  $\text{SiO}_2$ -assisted hydrophobic and hydrophilic treatment on poly(ethyl terephthalate) substrates and by introducing a Au NP-assisted recrystallization process. The massively patterned chalcogenide films prepared by this method have excellent optoelectronic properties, with sensitivities and detectivities of up to  $4.7 \text{ A W}^{-1}$  and  $6.3 \times 10^{12}$  jones, respectively, and on/off current ratios of  $5 \times 10^3$ . They also exhibit excellent electrical stability and flexural strength, demonstrating the imaging capability of PD arrays and the role of optical sensing in future optical imaging, digital display, and artificial electronic skin scenarios with versatile application potential.

**5.1.5 Gas sensors.** Condition monitoring and component analysis of human respiration are clinically important in reducing the high mortality rate due to respiratory arrest and pre-diagnosis of chronic diseases. Real-time wireless respiratory

monitoring and biomarker analysis offer an attractive prospect for non-invasive telemedicine, *e.g.*, for timely prevention of respiratory arrest or early diagnosis of chronic diseases.<sup>151–153</sup> Gas detection in flexible electronic devices requires novel materials with excellent sensing properties that are mechanically strong, flexible, low-cost and sustainable. Using LM ink, Huang *et al.*<sup>154</sup> prepared an LM epidermal electrode with high flexibility and high skin-fitting properties, and used the electrode as a carrier electrode for a tin disulfide sensing material to construct a wearable device for human respiration monitoring that can be directly attached to human skin. The device has high sensitivity and specificity for water vapor and nitric oxide exhaled by the human body, and can realize real-time monitoring of different respiratory states of the human body, as well as the alarm of high exhaled nitric oxide concentration. By pairing the data processing and analysis system with the Bluetooth transmission module, the electrical signal changes caused by the airflow in the middle of the human body can be transmitted to the mobile terminal in real time, realizing the real-time monitoring of multi-patient respiratory status. This work, as a portable wireless respiratory monitoring device, provides technical support for future cloud-based health monitoring, telemedicine and other fields.

Laser induced graphene (LIG) has attracted much attention due to its ability to synthesize porous graphene simply and rapidly. Stanford *et al.*<sup>155</sup> utilized a  $10.6 \mu\text{m}$   $\text{CO}_2$  laser to laser-prepare LIG-based gas sensors on a PI substrate, which senses gases based on thermal conductivity. During operation, an electrical potential is applied to the gas sensor, resulting in the heating of a highly resistive LIG channel. LIG has a high surface area of  $\sim 350 \text{ m}^2 \text{ g}^{-1}$  and the high thermal conductivity properties of graphene. LIG-based embeddable sensors can be integrated into composites to realize electronically functional building materials. Noteworthy, the sensor has an excellent fast response, which is attributed to the large surface area of LIG and its high thermal conductivity compared to common filament materials. The flexible and embeddable gas sensor demonstrates the ability to determine gas composition and represents a step towards realizing “smart” composite building materials.

Self-powered sensors are crucial in the field of wearable devices and the Internet of Things (IoT). Wang *et al.*<sup>132</sup> prepared an organ-like  $\text{Ti}_3\text{C}_2\text{T}_x$  MXene/metal-organic framework-derived copper oxide (CuO) gas sensor using latex- and polytetrafluoroethylene-based friction electro-nanogenerators (TENGs) as the driving force for ammonia ( $\text{NH}_3$ ) detection at room temperature. The open-circuit voltage and short-circuit current generated by the prepared TENG could reach peak-to-peak values of 810 V and  $34 \mu\text{A}$ , respectively. The self-powered  $\text{NH}_3$  sensor driven by the TENG showed excellent response ( $\sim 24.8$ ) at room temperature and could be used for the detection of pork deterioration (Fig. 10e). Zhang *et al.*<sup>156</sup> constructed a respiration sensor that can detect ammonia at the ppb level based on a soft-hard interface design of biocompatible seaweed fabric and nanosheet-assembled bismuth oxide structures after heat treatment. Utilizing abundant defect sites and surface chemical state changes, the flexible sensor can operate at room

temperature with ultra-high response, short response/recovery time, high selectivity, small detection limit, and good immunity to interference even after repetitive mechanical bending and long-term fatigue. It offers the prospect of early warning of ammonia leakage in chemical plants. Wang *et al.*<sup>157</sup> developed a TENG based on polyvinyl alcohol/silver (PVA/Ag) nanofibers for human respiration, motion and harmful gas monitoring. The PVA/Ag nanofiber film prepared by an electrostatic spinning technique as a high-performance friction electric material greatly improved the output performance of the TENG. A multifunctional self-powered detection system for wind direction and wind-loaded NO<sub>2</sub> was developed by integrating four TENGs with a gas sensor, which can be used to trace the source of harmful gases. This wind-powered self-powered sensor system provides a sustainable, maintenance-free detection platform with great potential for applications in environmental monitoring.

## 5.2 Flexible energy storage

Advances in flexible, wearable, and portable electronic devices are driving research in fabrication techniques, improved materials, and nanoscale morphology control, inspiring a relentless quest for advanced power sources that are multifunctional, sustainable, and highly stable.<sup>158,159</sup> With the booming development of wearable and portable electronics, there is an urgent need for flexible power supply systems with strong mechanical flexibility and high energy storage performance under various mechanical deformation conditions. In recent years, rapid progress has been made in material exploration, structural design, fabrication methods and integrated assembly of flexible energy storage devices.<sup>160,161</sup> Currently, carbon-based materials, including CNTs, graphene and its composites, MXenes, *etc.*, are replacing traditional metal films as collectors and are loaded with active substances for the preparation of bendable flexible batteries and supercapacitors.<sup>162,163</sup> “Paper electrodes”, sponges, porous frames, coil springs, and a variety of other interesting electrode structure designs have also contributed to the development of flexible energy storage devices.

**5.2.1 Batteries.** Flexible batteries are ductile, shock-resistant, and lightweight, and have significant market potential for integration into building and wearable electronics applications.<sup>164–166</sup> Flexible electrode materials are soft and flexible, and the surge in demand from new markets makes it likely that standard hard batteries will gradually decline.<sup>167–169</sup> Although some strategies can realize electrode flexibility, the cells produced have low specific capacity and poor performance. Therefore, three-dimensional electrode structures such as array structures, linear structures, and porous supports have emerged.

Silicon wafers are the most commonly used semiconductor substrate material in rigid electronic devices, and are used to manufacture about 95% of the solar cells in the current photovoltaic market. Due to their own natural brittleness, it is difficult to integrate them as functional units into flexible electronic devices. Amorphous silicon-derived complex films

are flexible, but their low power conversion efficiency (PCE) and unstable performance limit their large-scale application. Liu *et al.*<sup>170</sup> proposed a method to passivate the pyramidal structure at the wafer edges to improve the flexibility of silicon wafers, which can be used to prepare flexible solar cells (Fig. 11a). This method is suitable for fabricating large-scale, foldable crystalline silicon (c-Si). With the help of an advanced spherical aberration-corrected transmission electron microscopy characterization technique and geometric phase analysis (GPA) method, the deep-rooted mechanism of the edge-passivated silicon substrate with flexible features was verified. The cell maintained 100% power conversion efficiency after about 1000 bending cycles. In addition, it retained 96.03% of its power after 20 minutes of exposure to airflow when connected to a soft air pocket, which simulates the wind force in a violent storm. In the future, the team will attempt to further reduce the bending radius of the wafers by optimizing the angle at which the wafer's edges are cut, which will hopefully further advance applications such as a self-powered aircraft. Shu *et al.*<sup>171</sup> synthesized three-dimensional carbon nanosheets with highly branched CNTs and cobalt active sites (CoCNTs/PNAs) by rapid self-assembly pyrolysis (Fig. 11b). The hierarchical structure of the interconnected nanosheet aggregates of CNTs will promote efficient electron transfer and ion diffusion, which will enhance the electrocatalytic performance. n-Doped graphitic carbon layers with confinement effect can protect the cobalt nanoparticles from corrosive leaching, which optimizes the electronic structure and stability. A rechargeable zinc–air battery (ZAB) based on this electrolyte has a maximum power density of 371.6 mW cm<sup>−2</sup> and excellent cycling endurance (more than 2000 h). This work will open a new avenue to modulate metal–carbon support interactions for functional electrocatalysis through hierarchical porous structure design. Wang *et al.*<sup>174</sup> successfully prepared a novel conductive aqueous adhesive for high-strength, flexible and thick cathode/anode by interweaving CNTs in cellulose nanosheets. The adhesive has an ultrathin 2D reticulated nanosheet structure, which exhibits a novel “point-to-point” bonding mode with the active material. The flexible cell obtained by assembling it with the electrodes obtained an ultra-high surface capacity of 12.1 mA h cm<sup>−2</sup> and a good specific capacity (141 mA h g<sup>−1</sup>). This cellulose-based adhesive system is ideal for advanced high-performance functional devices, especially flexible and high-energy batteries.

**5.2.2 Supercapacitors.** Flexible supercapacitors (FSCs) are promising energy storage devices for flexible electronic devices. They have attracted great attention for their excellent flexibility, fast charging and discharging capability, and durable cycling stability. Compared with flexible batteries, it is relatively easy to design electrode structures for flexible supercapacitors, which mainly include two-dimensional (two-dimensional interlayer flexible electrode structure and two-dimensional planar electrode structure) and three-dimensional structures, such as the wave/block structure, line structure, and fabric structure.<sup>175–177</sup> Reasonable selection of electrode materials and structure optimization can significantly improve the electrochemical and mechanical properties of FSCs. Choi *et al.*<sup>172</sup> designed a new solid-state flexible supercapacitor consisting of activated



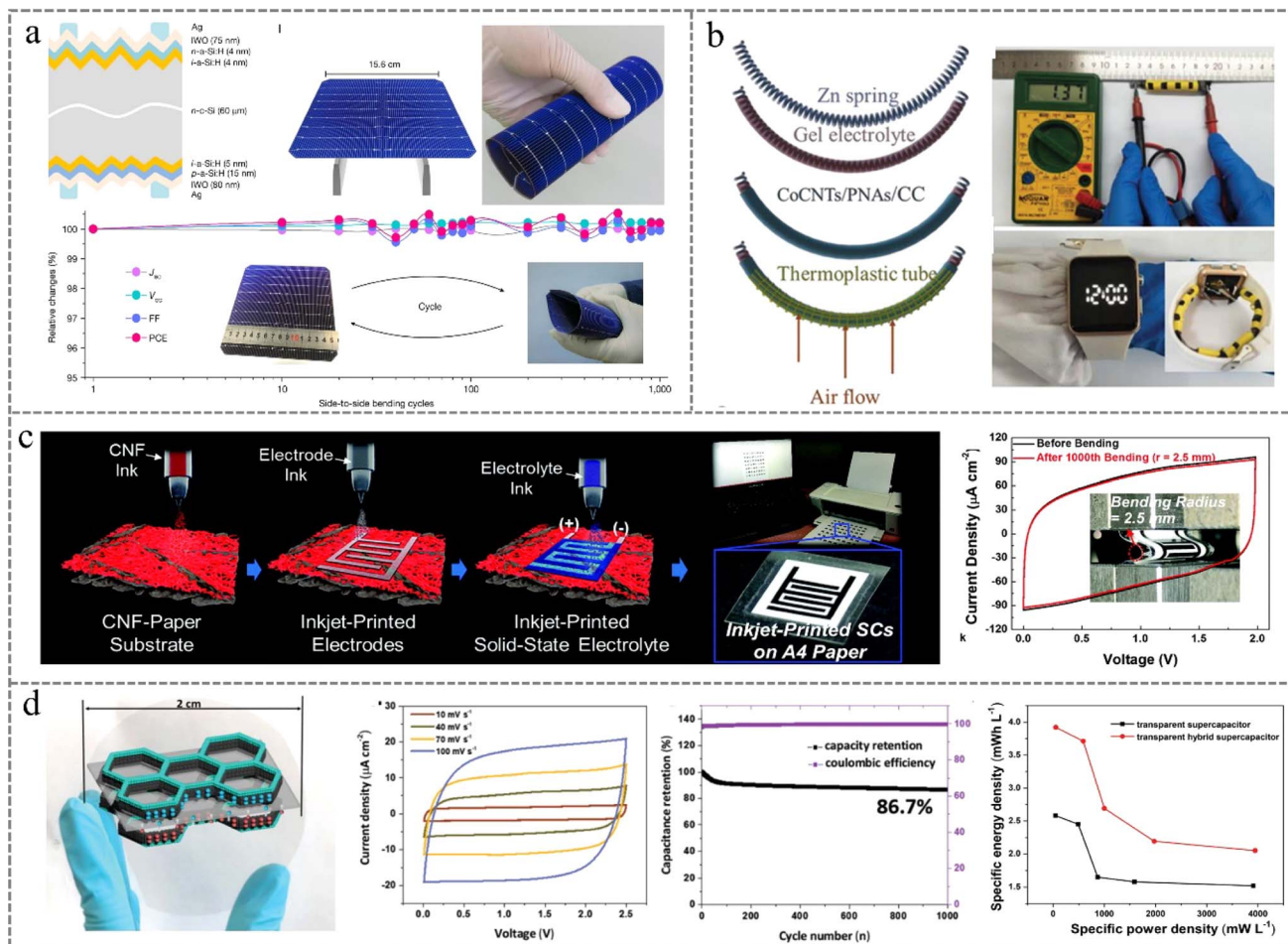


**Fig. 11** (a) Flexible solar cells based on foldable silicon wafers with passivated edges. Reproduced with permission from ref. 170. This is an open access article. (b) Graded porous N-doped carbon for high-performance rechargeable flexible zinc–air batteries. Reproduced with permission from ref. 171. Copyright©2023, Wiley. (c) Paper-based solid-state flexible supercapacitors based on full inkjet printing technology. Reproduced with permission from ref. 172. Copyright©2023, Royal Society of Chemistry. (d) Transparent flexible film supercapacitors and hybrid supercapacitors based on micro-molding technology. Reproduced with permission from ref. 173. Copyright©2020, Wiley.

charcoal/CNTs and ionic liquids/ultraviolet-cured polymer solid electrolytes, and the whole fabrication process can be done directly on A4 paper using a commercial desktop inkjet printer (Fig. 11c). The inkjet-printed paper-based all-solid-state flexible supercapacitors showed no significant decrease in capacitance value ( $100 \text{ mF cm}^{-2}$ ) after more than 10 000 charge/discharge cycles, and the devices did not show any mechanical damage after 2000 bending cycles, and the performance was stable. Liu *et al.*<sup>173</sup> developed a micro-molding method for different materials to prepare transparent Ag/porous carbon electrodes with a hexagonal lattice structure (Fig. 11d). Based on these electrodes, thin-film and hybrid transparent supercapacitors were prepared. Compared with the film-type supercapacitors, the hybrid capacitors exhibit higher transparency, longer cycle life, and higher energy density and power density. This micro-molding method is well suited for the assembly of nano-/micrometer-scale collectors and active materials, and promotes the development of transparent electrodes for next-generation flexible energy storage devices. Conventional graphene

synthesis is costly, has a long process time and is not environmentally friendly. This makes it difficult for graphene-based flexible supercapacitors to gain a cost advantage, so new synthesis strategies need to be developed. Li *et al.*<sup>178</sup> obtained graphene flakes by electrochemical exfoliation and coated them on commercial paper, and then deposited PANI nanorods by electrochemical deposition to obtain a highly conductive flexible graphene composite supercapacitor (PANI-GP). The capacitor has a face capacitance of up to  $176 \text{ mF cm}^{-2}$  in the three-electrode system at a current density of  $0.2 \text{ mA cm}^{-2}$ . Due to the pseudo-capacitive behavior of the conductive polymer PANI, the face capacitance of the PANI-GP is nearly ten times higher than that of the pure graphene supercapacitor, showing great potential for application in flexible energy storage devices.

Although the current prevalence of new energy vehicles has accelerated the rapid development of flexible batteries and supercapacitors, there are still many challenges to realizing the practical application of flexible energy storage devices. For example, how to ensure flexibility and high performance while

reducing costs, how to realize high-volume/mass production, and how to improve the cycling stability of energy storage devices.

### 5.3 Medical and healthcare

Flexible bioelectronic devices are valuable for applications in areas such as human health monitoring and human-computer interfaces, among which flexible electrodes have been widely studied, but in-depth research on them in improving signal quality and service life is still lacking. They may have the potential to solve problems that rigid electrodes cannot like better fit to the skin, muscle tissues and even brain tissues to reduce the body's immune response. Based on their invasiveness to the body, electrodes can be categorized into three main groups: invasive, semi-invasive and non-invasive.<sup>179</sup> A new technological solution that combines flexible electrodes with smart medical devices can monitor and analyze important physiological signals in the human body in real time, enabling disease prevention and early diagnosis.

**5.3.1 Brain-machine interfaces.** Flexible electrodes are an important development in the second generation of Brain-Machine Interfaces (BMIs), which have received much attention for their excellent performance and wide range of applications, stimulating people's imagination about the power and potential of controlling machines through their minds. Compared with traditional rigid electrodes, flexible electrodes have better adaptability and flexibility to better fit the complex shapes of the brain surface. With the development of flexible electronics and MEMS micro-nanofabrication technology, flexible brain-computer interface devices are increasingly being used to accurately capture high-density and high-information EEG signals, which provides a brand new tool for the study of neural loop function, confirming the diagnosis of lesions in brain regions, and neural decoding. Through molecular design, specific flexible materials can achieve mechanical and biological properties close to those of brain tissues, which is expected to solve the challenge of mechanical and chemical mismatch between rigid electronic components and soft brain tissues. Wang *et al.*<sup>180</sup> developed hydrophilic and electrically conductive 3,4-ethylenedioxythiophene nanoparticles (dPEDOT NPs) based on the domain-limited polymerization of double-bonded dopamine, and introduced them into the carrageenan (CA)-polydopamine (PDA)-polyacrylamide (PAM) interpenetrating hydrogel network, resulting in a conductive hydrogel (dPEDOT-CA-PDA-PAM) with ultra-soft, tissue-adhesive, and immune escape properties (Fig. 12a). By introducing conductive polymer nanoparticles with double-bonded dopamine domain-limited polymerization into the flexible hydrogel network, a conductive hydrogel with tissue adhesion and ultra-soft mechanical properties was successfully prepared and integrated with microscale electrodes to construct a flexible hydrogel-based brain-machine interface (BMI). The hydrogel BMI can overcome the mismatch of mechanical and biological properties with brain tissues, achieve immune escape at the level of *in vivo* inflammation, and is expected to be used as an implantable BMI for long-term monitoring of EEG signals. Ji *et al.*<sup>181</sup> formed

an optoelectronically integrated stretchable flexible brain-computer interface device by integrating a micro-LED chip inside a stretchable elastic substrate and combining it with ECoG electrodes (Fig. 12b). When the substrate stretching amount of the device is 10%, the serpentine wires on the surface of the device can be pasted on the surface of the elastic substrate intact; when the substrate stretching amount increases to 20%, the serpentine wires on the surface of the device are irreversibly partially debonded and leave the surface of the elastic substrate. In practice, a substrate stretch of 10% is sufficient to adapt to the deformation of brain tissue. This result demonstrates that the novel device has significant advantages in matching the mechanical stiffness of brain tissue and providing high-precision synchronized optical stimulation and electrical recording, which is of broad application value and has prospects for neuroscience and brain disease exploration.

The introduction of flexible materials to rationally design and model neural networks is one of the important applications of flexible electronic devices in medicine. The shift from rigid to flexible electrode materials requires the adaptation of modeling and characterization methods to understand and predict electrode performance. Lycke *et al.*<sup>184</sup> designed and developed ultra-flexible stimulated electron wires (StimNET electrodes) to simultaneously satisfy the requirements of robust charge injection and subcellular stability at the tissue electrode interface. To reduce the risk of crosstalk between nearby traces and to improve biocompatibility, polyimide (PI) was used as the matrix material. The effectiveness, resolution, stability and histocompatibility of neuromodulation were evaluated in a series of subsequent medical experiments. It was demonstrated that these tissue-integrated electrodes produced spatially restricted neuronal activation and elicited longitudinally stable behavioral detection at significantly reduced stimulus currents without neuronal degradation or glial scarring. This work resulted in the design of the thinnest and most flexible penetrating microelectrode array of StimNET electrodes currently available for use in a robust ICMS. During an 8 month period of intracortical implantation, up to 1.9 million pulses were stimulated *in vivo* per micro-contact on these devices without signs of biologic or abiotic failure. In this study, the StimNET electrodes delivered the same number of stimulation pulses *in vivo* as those used in recent human studies of ICMS, which were implanted for longer periods. These results suggest that the StimNET electrode has significant ultrafast oxidizability and a total thickness of 1 mm, supporting the long-term application of ICMS.

Neurotransmitters are chemical signals in the brain system and they play a key role in regulating the nervous system. Enabling the detection of neurotransmitters has important applications for clinical medicine, such as early screening for Parkinson's disease, addiction and major depression, among others. Methods used to detect biochemical signals *in vivo* currently include (i) genetically encoded fluorescent sensors and (ii) electrochemical analytical voltammetry. However, the detection of neurotransmitters *in vivo* remains a great challenge due to the poor tunability of the devices and the immunoinflammatory response that often accompanies them. Based

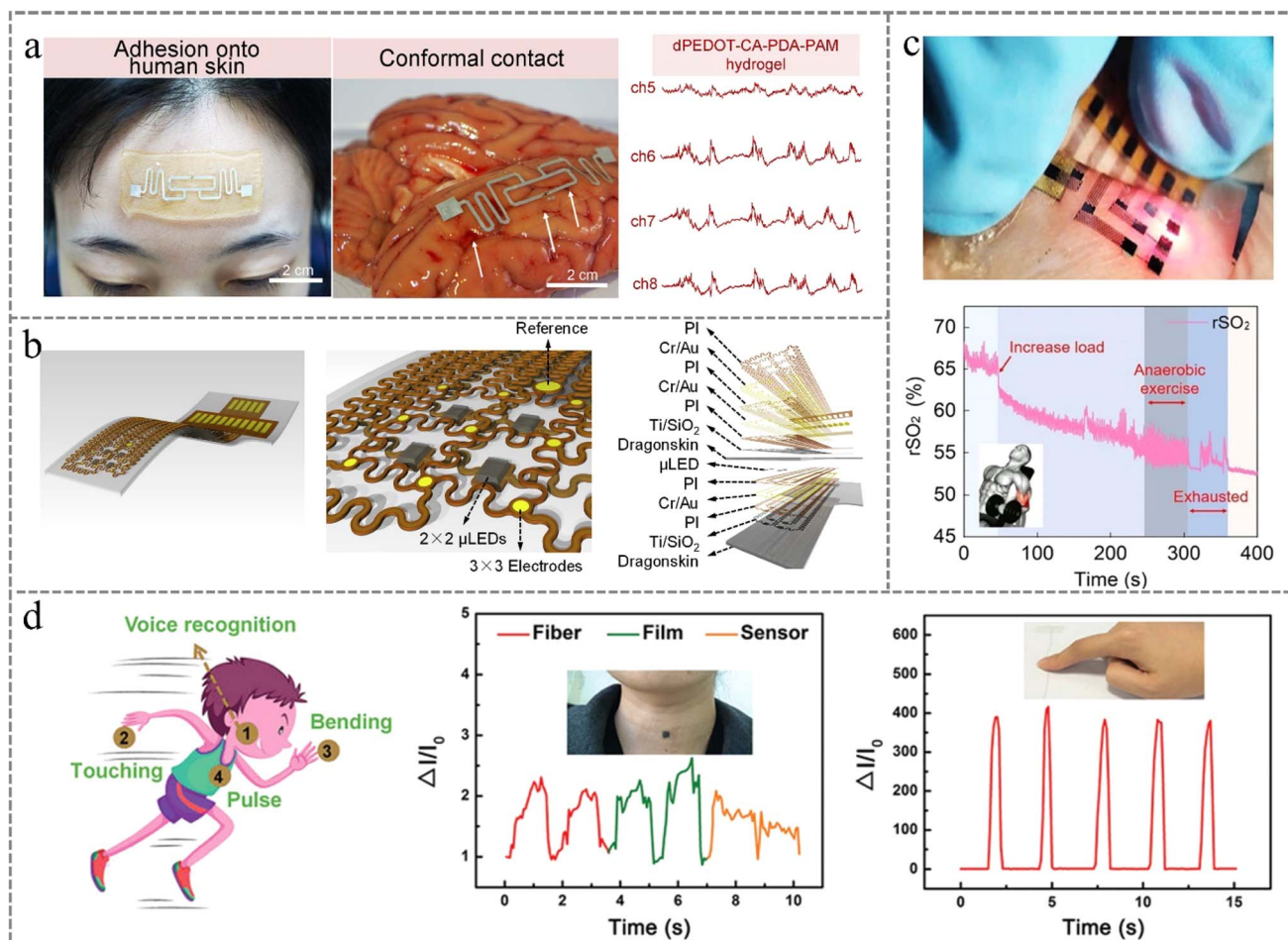


Fig. 12 (a) Bioadhesive and conductive hydrogel-based degradable brain-computer interface. Reproduced with permission from ref. 180. Copyright@2022, Elsevier. (b) Flexible and stretchable optoelectronic neural interface. Reproduced with permission from ref. 181. Copyright@2020, Elsevier. (c) Electronic skin for assessing local tissue hemodynamics. Reproduced with permission from ref. 182. This is an open access article. (d) High-performance electronic skin based on controlled assembly of active layer MXene nanosheets. Reproduced with permission from ref. 183. Copyright@2021, Wiley.

on fast scanning cyclic voltammetry (FSCV), Li *et al.*<sup>185</sup> chose graphene as the electrode material and prepared nanofiber networks by a laser carbonization process. A graphene nanofiber network decorated with transition metal nanoparticles and embedded with a flexible matrix was developed. It was ultimately combined into a flexible sensor for monitoring monoamine neurotransmitters and called NeuroString, which can be mounted on the brain or gut without interfering with the organ's own function. NeuroString works without interfering with the host's physiological activity and monitors two chemical signals with high fidelity. This implantable closed-loop system could be used to reprogram human brain chemicals in real time, enabling novel and powerful brain-computer interfaces.

**5.3.2 Artificial skin.** Artificial skin, with its ability to sense thermal stimuli without physical contact, will lead to innovative interactive experiences for smart robotics and augmented reality. Microscale actuators have given us the ability to precisely control the movements of fine microstructures, driving the application and development of micro-electromechanical systems (MEMS) in areas such as micro-

robotics, biomedical devices, and integrated electronics. Zhang *et al.*<sup>186</sup> used light-responsive liquid-crystal elastomers to construct responsive artificial skins, realizing passive polymer microstructures for mobile 3D printing. Under a programmed femtosecond laser, the liquid crystal elastomer skin is able to generate localized artificial goose bumps that precisely actuate the surrounding microstructures. This microdrive can tilt the micromirror to control light reflection and break down capillary force-induced self-assembled microstructures globally and locally. This work demonstrates the potential application of microdrive systems in information storage, providing precise, localized and controlled manipulation of microstructures and opening new opportunities for the development of programmable micromachines. Arterial oxygenation sensors based on optoelectronic volumetric pulse waves in the superficial arterial position have been used in a large number of applications in clinical diagnosis and daily life. Currently, the most commonly used methods for diagnosing and monitoring peripheral arterial disease are ankle-brachial index, partial pressure of oxygen, and CT angiography; however, these methods involve costly



measurements, complex instruments, and require the intervention of a professionally trained clinician. In addition, none of these methods address the need for remote end-cardiac tissue hemodynamic monitoring after the patient is discharged from the hospital. Xin *et al.*<sup>182</sup> introduced an ultralight, ultrathin biophotonic sensor with multi-vital parameter sensing capability for continuous hemodynamic monitoring and applied it to analyze a variety of clinical symptoms caused by PAD (Fig. 12c). The sensor was able to accurately, directly, and rapidly reflect tissue hemodynamic parameters, and the measurements were highly correlated with the results of ABI and CTA analyses. In patients with atherosclerosis and low lesion planes, the sensor showed the ability to correct false positives of the ABI. The skin photoelectric biosensor shows great potential for the study of organ tissue oxygen mediation, sports medicine, and AI monitoring of PAD.

MXenes are an emerging class of two-dimensional transition metal carbides and nitrides. Due to their excellent conductivity, flexibility and editability, they have been widely used in the field of flexible electronic skin. Fu *et al.*<sup>183</sup> deposited MXene materials onto the upper and lower surfaces of three-dimensional polyacrylonitrile (PAN) networks in turn by vacuum filtration technology to obtain a uniform  $\text{Ti}_3\text{C}_2\text{T}_x$  MXene electronic skin, and in this way piggybacked it into MXene/PAN flexible pressure sensors that can tightly adhere (Fig. 12d) to the skin to monitor the human body dynamics in real time, and has a high sensitivity of  $104.0 \text{ kPa}^{-1}$ , a fast response/recovery time (30/20 ms), and a low detection limit (1.5 Pa), which confirms its broad application prospects. Thermal sensing is a fundamental sensing process that enables people to better receive environmental signals and respond in time by sensing different temperatures. Thermal-aware electronic skin patches are flexible, portable, and heat-sensitive, and can assist people with real-time feedback of thermal stimulus signals. Guo *et al.* proposed a feasible strategy to integrate infrared detection technology into electronic skin sensing modes.<sup>187</sup> Flexible infrared detection patches based on tellurium-based thermoelectric multilayer films coupled with infrared-absorbing polyimide substrate photo-thermoelectricity were prepared and obtained. The multilayer heterostructure with alternating stacks of tellurium and copper telluride films resulted in a 250% increase in material conductivity without a significant decrease in the Seebeck coefficient. A dynamic temperature warning system for flexible robotic grippers was developed. The system is capable of recognizing noxious thermal stimuli in a non-contact manner, demonstrating practical applicability in real-world scenarios.

Flexible electrodes used in the medical field are usually made of biocompatible materials, which can effectively fit the skin, muscle tissues and even brain tissues, meeting the need for multiple bending and folding in surgery, reducing damage to the human body and increasing the safety of use. At the same time, good adhesion also minimizes signal loss and noise interference, thus improving signal quality. However, compared with rigid electrodes, there are still some shortcomings: (i) poor signal stability and reproducibility, easily affected by the environment (heartbeat, blood pressure, body temperature, *etc.*)

making the signal unstable or even invalid; (ii) the human body implantation is difficult and costly, and needs to take special methods and processes, which requires high requirements for medical skills and implantation equipment.

## 6. Conclusion and perspectives

Flexible electronics eliminate the discomfort of wearing them and the limitations on human motion monitoring due to rigid materials and metal parts. Specifically, the latest advances in wearable systems mainly lie in the compatibility of flexible electronics in contact with human skin, with research focusing on high flexibility, breathability, softness, biocompatibility, non-toxicity, *etc.*, thus solving problems such as skin allergy and inflammation, and realizing the ability to have real-time monitoring of human movement, biological signals, environmental factors, and other physical and chemical changes. From rollable computer screens to smart clothing and even biomedical monitoring devices, electronics will become increasingly flexible in the future. The rapid development of wearable and implantable devices, brain-computer interfaces, and bendable displays urgently requires electrodes that can match the flexibility of these systems. In this paper, we introduce the currently commonly used materials for preparing flexible electrodes, including flexible substrates (fibers/fabrics, hydrogels/aerogels, polymer films) and active materials (metals and derivatives, carbon-based materials, MXenes, MOFs, *etc.*). A brief overview of flexible electrode design ideas and preparation techniques is presented through printing, vacuum filtration, deposition, and electro/chemical plating. The applications of flexible electrodes in the fields of sensors, energy storage, and medical and health monitoring are also analyzed. However, it is not difficult to imagine that, as an emerging field, the current flexible electronics technology is still in its infancy, and its research and development process is still facing many difficulties and challenges of technological breakthroughs.

Firstly, the selection of flexible electrode materials. Many materials such as conductive polymers, graphene, *etc.*, although highly conductive, are prone to fracture, detachment, or even deprotonation spontaneous deactivation during the working process, leading to serious performance degradation, which makes it difficult to meet the electrode requirements. Moreover, the coefficient of thermal expansion of flexible materials tends to be high, which is susceptible to environmental factors such as temperature and humidity, and easily leads to the aging and failure of electronic devices. Therefore, how to develop new flexible materials to improve their strength, conductivity and stability has become one of the difficulties in manufacturing flexible electronics.

Secondly, the structural design of flexible electronic devices. Flexible electronic components are subjected to alternating stresses during repeated folding and bending, and are prone to cracking and failure over time. Compared with hard electronic products, the manufacturing process of flexible electronic devices needs to consider the plasticity, maneuverability and reproducibility of the material. The processing of flexible materials usually involves steps such as printing, deposition,

and filtering, which are constrained by process parameters, material properties, and equipment limitations, and can easily lead to unstable processes and difficult optimization of equipment parameters.

Thirdly, the stability and reusability of flexible electronic devices. Flexible electronic devices usually consist of multiple functional modules and components, which need to realize the effective integration and reliable connection of different materials and different processes. In the manufacturing process, attention needs to be paid to issues such as compatibility between materials and different interfaces, adhesion and stability of packaging. In addition, the long-term stability and reusability of flexible electronic devices are also factors that need to be focused on. Therefore, it is one of the technological breakthroughs in manufacturing flexible electrodes to develop a new and reliable electronic packaging technology to improve the integration and reliability of flexible electronics and extend their service life.

Finally, there is an issue of cost. Due to the high manufacturing complexity of flexible electronics, it is necessary to use some highly complex production processes such as microelectromechanical systems, nanofabrication and so on. Therefore, it is necessary to research a more efficient and convenient production process to better promote the industrialization of flexible electronics technology. At this stage, there is still a lack of reliable preparation processes to realize mass production, resulting in high production costs.

In summary, the difficulties in the large-scale fabrication of flexible electronic devices include challenges in the selection of flexible electrode materials, design and fabrication processes, device integration, applicability and cost issues. In order to overcome the difficulties, it is necessary to consider various aspects of material selection, electrode structure optimization, and packaging process, on the one hand, research and development of new flexible materials, exploring new applications of carbon-based materials, conductive biocompatible materials, *etc.*, to improve the strength, conductivity and stability of flexible materials, and on the other hand, optimizing the manufacturing process, adopting intelligent flexible electrode manufacturing equipment, realizing online monitoring and control of process parameters, and improving product quality and production efficiency, as well as strengthening the design and packaging technology of flexible electronic systems to improve integration and reliability.

## Conflicts of interest

There are no conflicts to declare.

## Acknowledgements

This work was supported by the Qingdao Natural Science Foundation, Youth Innovation Team Project of Shandong Province (No. 2021KJ018), and Taishan Scholar Program of Shandong Province (No. tsqn201812055).

## References

- 1 S. Huang, Y. Liu, Y. Zhao, Z. Ren and C. F. Guo, *Adv. Funct. Mater.*, 2018, **29**, 1805924.
- 2 A. K. Katiyar, A. T. Hoang, D. Xu, J. Hong, B. J. Kim, S. Ji and J.-H. Ahn, *Chem. Rev.*, 2023, **124**, 318–419.
- 3 X. Zhang, C. Jiang, J. Liang and W. Wu, *J. Mater. Chem. A*, 2021, **9**, 8099–8128.
- 4 K. Zeng, X. Shi, C. Tang, T. Liu and H. Peng, *Nat. Rev. Mater.*, 2023, **8**, 552–561.
- 5 B. C. K. Tee and J. Ouyang, *Adv. Mater.*, 2018, **30**, 1802560.
- 6 K. K. Pawar, A. Kumar, A. Mirzaei, M. Kumar, H. W. Kim and S. S. Kim, *Chemosphere*, 2024, **352**, 141234.
- 7 C. Zhang, J. Zhu, H. Lin and W. Huang, *Adv. Mater. Technol.*, 2018, **3**, 1700302.
- 8 K. Shang, J. Gao, X. Yin, Y. Ding and Z. Wen, *Eur. J. Inorg. Chem.*, 2021, **2021**, 606–619.
- 9 J. Zeng, P. Qi, Y. Wang, Y. Liu and K. Sui, *J. Hazard. Mater.*, 2021, **410**, 12463.
- 10 S. Wei, C. Wan and Y. Wu, *Green Chem.*, 2023, **25**, 3322–3353.
- 11 M. Luo, Y. Liu, W. Huang, W. Qiao, Y. Zhou, Y. Ye and L.-S. Chen, *Micromachines*, 2017, **8**, 12.
- 12 S. Yasami, S. Mazinani and M. Abdouss, *J. Energy Storage*, 2023, **72**, 108807.
- 13 F. Torrisi and T. Carey, *Nano Today*, 2018, **23**, 73–96.
- 14 M. Bigdeloo, A. Ehsani, S. Sarabadani and H. M. Shiri, *J. Energy Storage*, 2024, **80**, 110242.
- 15 D. Lei, N. Liu, T. Su, Q. Zhang, L. Wang, Z. Ren and Y. Gao, *Adv. Mater.*, 2022, **34**, 2110608.
- 16 J. Khan, A. Khan, B. Rubab, F. Jamshaid, A. A. Al-Kahtani and A. Dahshan, *Appl. Mater. Today*, 2023, **34**, 101906.
- 17 D. Chen, J. Liang and Q. Pei, *Sci. China: Chem.*, 2016, **59**, 659–671.
- 18 Y. Xiao, M. Wang, Y. Li, Z. Sun, Z. Liu, L. He and R. Liu, *Micromachines*, 2021, **12**, 1505.
- 19 J. S. Meena, S. B. Choi and J.-W. Kim, *Electron. Mater. Lett.*, 2022, **18**, 256–274.
- 20 Y. Zhao, B. Wang, J. Tan, H. Yin, R. Huang, J. Zhu, S. Lin, Y. Zhou, D. Jelinek, Z. Sun, K. Youssef, L. Voisin, A. Horrillo, K. Zhang, B. M. Wu, H. A. Collier, D. C. Lu, Q. Pei and S. Emaminejad, *Science*, 2022, **378**, 1222–1227.
- 21 Y. Zhang, J. Riexinger, X. Yang, E. Mikhailova, Y. Jin, L. Zhou and H. Bayley, *Nature*, 2023, **620**, 1001–1006.
- 22 J. Kim, G. Zhang, M. Shi and Z. Suo, *Science*, 2021, **374**, 212–216.
- 23 H. Yuk, B. Lu and X. Zhao, *Chem. Soc. Rev.*, 2019, **48**, 1642–1667.
- 24 E. Lai, X. Yue, W. E. Ning, J. Huang, X. Ling and H. Lin, *Front. Chem.*, 2019, **7**, 660.
- 25 Q. Han, C. Zhang, T. Guo, Y. Tian, W. Song, J. Lei, Q. Li, A. Wang, M. Zhang, S. Bai and X. Yan, *Adv. Mater.*, 2023, **35**, 12.
- 26 J. Wang, Q. Zhou, A. Wang, Z. Zhu, K. Moses, T. Wang, P. Li and W. Huang, *Adv. Funct. Mater.*, 2024, **34**, 2309704.

- 27 C. Wang, J. Zhang, X. Wang, C. Lin and X. S. Zhao, *Adv. Funct. Mater.*, 2020, **30**, 2002629.
- 28 R. Bao, S. Wang, X. Liu, K. Tu, J. Liu, X. Huang, C. Liu, P. Zhou and S. Liu, *Nat. Commun.*, 2024, **15**, 1327.
- 29 L. Yan, C. Zhao, Y. Wang, Q. Qin, Z. Liu, Y. Hu, Z. Xu, K. Wang, X. Jiang, L. Han and X. Lu, *Nano Today*, 2023, **51**, 101934.
- 30 Q. Liang, X. Xia, X. Sun, D. Yu, X. Huang, G. Han, S. M. Mugo, W. Chen and Q. Zhang, *Adv. Sci.*, 2022, **9**, 2201059.
- 31 Y. Wu, C. An, Y. Guo, Y. Zong, N. Jiang, Q. Zheng and Z.-Z. Yu, *Nano-Micro Lett.*, 2024, **16**, 118.
- 32 P. Wang, D. Fan, L. Gai, B. Hu, P. Xu, X. Han and Y. Du, *J. Mater. Chem. A*, 2024, **12**, 8571–8582.
- 33 X. Du and K. Zhang, *Nano Energy*, 2022, **101**, 107600.
- 34 K. Zhang, X. Shi, H. Jiang, K. Zeng, Z. Zhou, P. Zhai, L. Zhang and H. Peng, *Nat. Protoc.*, 2024, **19**, 1557–1589.
- 35 J.-W. Zhang, Y. Zhang, Y.-Y. Li and P. Wang, *Polym. Rev.*, 2021, **62**, 65–94.
- 36 C. Sun, Z. Han, X. Wang, B. Liu, Q. Li, H. Li, J. Xu, J. M. Cao and X. L. Wu, *Adv. Funct. Mater.*, 2023, **33**, 2305606.
- 37 S. Lee and G.-H. An, *Adv. Fiber Mater.*, 2023, **5**, 1749–1758.
- 38 T. Li, H. Chen, Z. Chen, Z. Xue, X. Zhang and B. Hui, *ACS Sustain. Chem. Eng.*, 2023, **11**, 14549–14558.
- 39 S. Woo, D. Nam, W. Chang, Y. Ko, S. Lee, Y. Song, B. Yeom, J. H. Moon, S. W. Lee and J. Cho, *Small*, 2021, **17**, 2007579.
- 40 M. L. R. Liman, M. T. Islam and M. M. Hossain, *Adv. Electron. Mater.*, 2021, **8**, 2100578.
- 41 J. Wang, X. Y. Thow, H. Wang, S. Lee, K. Voges, N. V. Thakor, S. C. Yen and C. Lee, *Adv. Healthcare Mater.*, 2017, **7**, 1700987.
- 42 H. Moon, J.-W. Jang, S. Park, J.-H. Kim, J. S. Kim and S. Kim, *Sens. Actuators, B*, 2024, **401**, 135099.
- 43 P. Xie, W. Yuan, X. Liu, Y. Peng, Y. Yin, Y. Li and Z. Wu, *Energy Storage Mater.*, 2021, **36**, 56–76.
- 44 Q. Ge, J. Chu, W. Cao, F. Yi, Z. Ran, Z. Jin, B. Mao, Z. Li and K. S. Novoselov, *Adv. Funct. Mater.*, 2022, **32**, 2205934.
- 45 J. Miao and T. Fan, *Carbon*, 2023, **202**, 495–527.
- 46 D. Koo, S. Jung, J. Seo, G. Jeong, Y. Choi, J. Lee, S. M. Lee, Y. Cho, M. Jeong, J. Lee, J. Oh, C. Yang and H. Park, *Joule*, 2020, **4**, 1021–1034.
- 47 J. Suo, Y. Liu, J. Wang, M. Chen, K. Wang, X. Yang, K. Yao, V. A. L. Roy, X. Yu, W. A. Daoud, N. Liu, J. Wang, Z. Wang and W. J. Li, *Adv. Sci.*, 2024, **11**, 2305025.
- 48 Y. Zheng, W. Zhao, D. Jia, Y. Liu, L. Cui, D. Wei, R. Zheng and J. Liu, *Chem. Eng. J.*, 2020, **387**, 124161.
- 49 B. Li, S. Zhan, H. Wang, B. Hou and G. A. J. Amaratunga, *Adv. Mater. Technol.*, 2020, **5**, 8940–8952.
- 50 W. Jiang, S. Lee, K. Zhao, K. Lee, H. Han, J. Oh, H. Lee, H. Kim, C. M. Koo and C. Park, *ACS Nano*, 2022, **16**, 9203–9213.
- 51 S. Lee, E. H. Kim, S. Yu, H. Kim, C. Park, S. W. Lee, H. Han, W. Jin, K. Lee, C. E. Lee, J. Jang, C. M. Koo and C. Park, *ACS Nano*, 2021, **15**, 8940–8952.
- 52 M. Dong, P. Chen, K. Zhou, J. B. Marroquin, M. Liu, S. Thomas, H. A. Coleman, D. Li, J. B. Fallon, M. Majumder, H. C. Parkington and J. S. Forsythe, *Chem. Eng. J.*, 2023, **478**, 147067.
- 53 J. M. Lee, Y.-W. Pyo, Y. J. Kim, J. H. Hong, Y. Jo, W. Choi, D. Lin and H.-G. Park, *Nat. Commun.*, 2023, **14**, 7088.
- 54 Y. Cai, Y. Wang, L. Cheng, S. Guo, T. Liu, Z. Hu, H. Yu, D. Chen, Y. Li and H. Yuan, *J. Energy Storage*, 2023, **73**, 109179.
- 55 L. Gao, S. Lv, Y. Shang, S. Guan, H. Tian, Y. Fang, J. Wang and H. Li, *Nano Lett.*, 2023, **24**, 829–835.
- 56 H. Kazari, E. Pajootan, M. Sowa, S. Coulombe and P. Hubert, *J. Energy Storage*, 2023, **64**, 107049.
- 57 H. Zhou, S. Wu, H. Wang, Y. Li, X. Liu and Y. Zhou, *J. Hazard. Mater.*, 2021, **402**, 124023.
- 58 C. Xu, C. Jin, J. Liu, K. Song, X. Wang and X. Gong, *J. Energy Storage*, 2021, **36**, 102394.
- 59 X. Zhao, Y. Huang, H. Jiang, X. Liu, M. Yu and M. Zong, *Carbon*, 2024, **224**, 119063.
- 60 L. Chen, Y. Yuan, R. Orenstein, M. Yanilmaz, J. He, J. Liu, Y. Liu and X. Zhang, *Energy Storage Mater.*, 2023, **60**, 102817.
- 61 X. Zhao, L. Tian, T. Liu, H. Liu, S. Wang, X. Li, O. Fenwick, S. Lei and W. Hu, *J. Mater. Chem. A*, 2019, **7**, 1509–1518.
- 62 V. Martinez-Agramunt, T. Eder, H. Darmandeh, G. Guisado-Barrios and E. Peris, *Angew Chem. Int. Ed. Engl.*, 2019, **58**, 5682–5686.
- 63 H. Zhang, W. Wu, X. Yu, M. Tong, J. Zhou, J. Cao, P. Gao, J. Zhao, H. Xu and H. Ma, *Carbon*, 2019, **142**, 411–419.
- 64 X. Liu, Y. Ying and J. Ping, *Biosens. Bioelectron.*, 2020, **167**, 112495.
- 65 K. Paneer Selvam, T. Nagahata, K. Kato, M. Koreishi, T. Nakamura, Y. Nakamura, T. Nishikawa, A. Satoh and Y. Hayashi, *Biomater. Res.*, 2020, **24**, 18.
- 66 X. Wang, A. A. Aboalhassan, C. Zhu, L. Zhang, G. Li, J. Yan, J. Yu and B. Ding, *Adv. Mater. Interfaces*, 2022, **9**, 2201231.
- 67 D. Li, F. Raza, Q. Wu, X. Zhu and A. Ju, *ACS Appl. Nano Mater.*, 2022, **5**, 14630–14638.
- 68 Y. Wang, H. Tang, Q. Xie, J. Liu, S. Sun, M. Zhou and Y. Zhang, *Chem. Eng. J.*, 2024, **481**, 148558.
- 69 Z. Zhao, Z. Zhang, Y. Zhao, J. Liu, C. Liu, Z. Wang, G. Zheng, G. Huang and Y. Mei, *Adv. Funct. Mater.*, 2019, **29**, 1906365.
- 70 Z. Wu, L. Wei, S. Tang, Y. Xiong, X. Qin, J. Luo, J. Fang and X. Wang, *ACS Nano*, 2021, **15**, 18880–18894.
- 71 Y. An, Y. Tian, H. Shen, Q. Man, S. Xiong and J. Feng, *Energy Environ. Sci.*, 2023, **16**, 4191–4250.
- 72 Y. Li, W. Cao, Z. Liu, Y. Zhang, Z. Chen and X. Zheng, *Carbon Energy*, 2024, **6**, e530.
- 73 J. Chen, Z. Li, F. Ni, W. Ouyang and X. Fang, *Mater. Horiz.*, 2020, **7**, 1828–1833.
- 74 D. Wang, D. Zhang, M. Tang, H. Zhang, T. Sun, C. Yang, R. Mao, K. Li and J. Wang, *Nano Energy*, 2022, **100**, 107509.
- 75 D. Wang, D. Zhang, P. Li, Z. Yang, Q. Mi and L. Yu, *Nano-Micro Lett.*, 2021, **13**, 57.
- 76 L. Lyu, W. Hooch Antink, Y. S. Kim, C. W. Kim, T. Hyeon and Y. Piao, *Small*, 2021, **17**, 2101974.
- 77 H. Zhang, H. Ning, J. Busbee, Z. Shen, C. Kiggins, Y. Hua, J. Eaves, J. D. III, T. Shi, Y.-T. Shao, J.-M. Zuo, X. Hong,



- Y. Chan, S. Wang, P. Wang, P. Sun, S. Xu, J. Liu and P. V. Braun, *Sci. Adv.*, 2017, **3**, e1602427.
- 78 S. Huang, Y. Liu, F. Yang, Y. Wang, T. Yu and D. Ma, *Environ. Chem. Lett.*, 2022, **20**, 3005–3037.
- 79 Y. Peng, H. Peng, Z. Chen and J. Zhang, *Adv. Mater.*, 2023, **36**, 2305707.
- 80 F. Li, W. Lei, Y. Wang, X. Lu, S. Li, F. Xu, Z. He, J. Liu, H. Yang, Y. Wu, J. Shang, Y. Liu and R.-W. Li, *npj Flexible Electron.*, 2023, **7**, 31.
- 81 D. A. Kwon, S. Lee, C. Y. Kim, I. Kang, S. Park and J.-W. Jeong, *Sci. Adv.*, 2024, **10**, eadn1186.
- 82 Y. Zhao, B. Wang, J. Tan, H. Yin, R. Huang, J. Zhu, S. Lin, Y. Zhou, D. Jelinek, Z. Sun, K. Youssef, L. Voisin, A. Horrillo, K. Zhang, B. M. Wu, H. A. Collier, D. C. Lu, Q. Pei and S. Emaminejad, *Science*, 2022, **378**, 1222–1227.
- 83 G. Yang, X. Zheng, J. Li, C. Chen, J. Zhu, H. Yi, X. Dong, J. Zhao, L. Shi, X. Zhang, Y. Qin, Z. Gu and Z. Li, *Adv. Funct. Mater.*, 2024, **34**, 2401415.
- 84 J. E. Ten Elshof, H. Yuan and P. Gonzalez Rodriguez, *Adv. Energy Mater.*, 2016, **6**, 1600355.
- 85 S. A. Delbari, L. S. Ghadimi, R. Hadi, S. Farhoudian, M. Nedaie, A. Babapoor, A. Sabahi Namini, Q. V. Le, M. Shokouhimehr, M. Shahedi Asl and M. Mohammadi, *J. Alloys Compd.*, 2021, **857**, 158281.
- 86 Y. Huang, J. Liu, Q. Huang, Z. Zheng, P. Hiralal, F. Zheng, D. Ozgit, S. Su, S. Chen, P.-H. Tan, S. Zhang and H. Zhou, *npj Flexible Electron.*, 2018, **21**, 2.
- 87 X. Han, G. Xiao, Y. Wang, X. Chen, G. Duan, Y. Wu, X. Gong and H. Wang, *J. Mater. Chem. A*, 2020, **8**, 23059–23095.
- 88 J. Zhang, L. Wang, Y. Xue, I. M. Lei, X. Chen, P. Zhang, C. Cai, X. Liang, Y. Lu and J. Liu, *Adv. Mater.*, 2022, **35**, 2209324.
- 89 P. Wang, K. Liu, X. Wang, Z. Meng, Z. Xin, C. Cui, F. Quan, K. Zhang and Y. Xia, *J. Mater. Chem. A*, 2022, **10**, 15776–15784.
- 90 K.-K. Liu, Z.-J. Guan, M. Ke and Y. Fang, *ACS Cent. Sci.*, 2023, **9**, 805–815.
- 91 K. Liu, M. Zhang, X. Du, A. Zhou, B. Hui, Y. Xia and K. Zhang, *Nano Res.*, 2022, **16**, 1296–1303.
- 92 D. Gao, P. Zhao, J. Liu, Y. Zhou, B. Lyu, J. Ma and L. Shao, *Adv. Powder Technol.*, 2021, **32**, 3954–3963.
- 93 D. Cai, Z. Yang, R. Tong, H. Huang, C. Zhang and Y. Xia, *Small*, 2023, **20**, 2305778.
- 94 Q. Lu, T. Su, Z. Shang, D. Jin, Y. Shu, Q. Xu and X. Hu, *Biosens. Bioelectron.*, 2021, **184**, 113229.
- 95 Y. Wu, Y. Luo, P. K. Chu and C. Menon, *Nano Energy*, 2023, **111**, 108427.
- 96 B. Yao, J. Zhang, T. Kou, Y. Song, T. Liu and Y. Li, *Adv. Sci.*, 2017, **4**, 1700107.
- 97 L. Liu, Z. Ji, S. Zhao, Q. Niu and S. Hu, *J. Mater. Chem. A*, 2021, **9**, 6172–6179.
- 98 N. R. Tanguy, K. Khorsand Kazemi, J. Hong, K.-C. Cheung, S. Mohammadi, P. Gnanasekar, S. S. Nair, M. H. Zarifi and N. Yan, *Carbohydr. Polym.*, 2022, **278**, 118920.
- 99 S. Kumar and Y. Seo, *Small Methods*, 2023, **8**, 2300908.
- 100 D. Wang, Y. Zhang, X. Lu, Z. Ma, C. Xie and Z. Zheng, *Chem. Soc. Rev.*, 2018, **47**, 4611–4641.
- 101 L. Meng, W. Wang, B. Xu, J. Qin, K. Zhang and H. Liu, *ACS Nano*, 2023, **17**, 4180–4192.
- 102 R. Y. Tay, Y. Song, D. R. Yao and W. Gao, *Mater. Today*, 2023, **71**, 135–151.
- 103 Y. Zhao, C. Chen, B. Lu, X. Zhu and G. Gu, *Adv. Funct. Mater.*, 2023, **34**, 2312480.
- 104 X. Zhu, M. Liu, X. Qi, H. Li, Y. F. Zhang, Z. Li, Z. Peng, J. Yang, L. Qian, Q. Xu, N. Gou, J. He, D. Li and H. Lan, *Adv. Mater.*, 2021, **33**, 2007772.
- 105 X. Chen, W. Jian, Z. Wang, J. Ai, Y. Kang, P. Sun, Z. Wang, Y. Ma, H. Wang, Y. Chen and X. Feng, *Sci. Adv.*, 2023, **9**, eadi0357.
- 106 F. Ershad, M. Houston, S. Patel, L. Contreras, B. Koirala, Y. Lu, Z. Rao, Y. Liu, N. Dias, A. Haces-Garcia, W. Zhu, Y. Zhang, C. Yu and P. Sharma, *PNAS Nexus*, 2023, **2**, 1–14.
- 107 Z. Lv, C. Wang, C. Wan, R. Wang, X. Dai, J. Wei, H. Xia, W. Li, W. Zhang, S. Cao, F. Zhang, H. Yang, X. J. Loh and X. Chen, *Adv. Mater.*, 2022, **34**, 2202877.
- 108 M. S. Saleh, S. M. Ritchie, M. A. Nicholas, H. L. Gordon, C. Hu, S. Jahan, B. Yuan, R. Bezbaruah, J. W. Reddy, Z. Ahmed, M. Chamanzar, E. A. Yttri and R. P. Panat, *Sci. Adv.*, 2022, **8**, eabj4853.
- 109 L. J. Sutherland, D. Vak, M. Gao, T. A. N. Peiris, J. Jasieniak, G. P. Simon and H. Weerasinghe, *Adv. Energy Mater.*, 2022, **12**, 2202142.
- 110 W.-B. Zhu, F.-L. Yi, P. Huang, H. Zhang, Z.-H. Tang, Y.-Q. Fu, Y.-Y. Wang, J. Huang, G.-H. Dong, Y.-Q. Li and S.-Y. Fu, *J. Mater. Chem. A*, 2021, **9**, 26758–26766.
- 111 Y. Jiang, J. Ou, Z. Luo, Y. Chen, Z. Wu, H. Wu, X. Fu, S. Luo and Y. Huang, *Small*, 2022, **18**, 25.
- 112 B. Lyu, M. Kim, H. Jing, J. Kang, C. Qian, S. Lee and J. H. Cho, *ACS Nano*, 2019, **13**, 11392–11400.
- 113 A. Kaffle, M. Kumar, D. Gupta and T. C. Nagaiah, *J. Mater. Chem. A*, 2021, **9**, 24299–24307.
- 114 J. Zhang, W. Zhang, H. Wei, J. Tang, D. Li and D. Xu, *Nano Energy*, 2023, **105**, 108023.
- 115 Y. Guo, X. Zhang, F. Jiang, X. Tian, J. Wu and J. Yan, *Adv. Funct. Mater.*, 2024, **34**, 2313645.
- 116 B. Yao, Y. Yan, Q. Cui, S. Duan, C. Wang, Y. Du, Y. Zhao, D. Wu, S. Wu, X. Zhu, T. Hsiai and X. He, *Matter*, 2022, **5**, 4407–4424.
- 117 J. Gou, Y. Wang, H. Zhang, Y. Tan, Y. Yu, C. Qu, J. Yan, H. Zhang and X. Li, *Sci. Bull.*, 2020, **65**, 917–925.
- 118 Y. Pan, Y. Zhang, X. Shi, D. Li, X. Xu, B. Xiao, Y. Piao, J. Xiang, S. Shao, F. C.-Y. Ho, Y. Shen, A. P. Zhang and J. Tang, *Sci. Bull.*, 2023, **68**, 2779–2792.
- 119 W. Hao, R. Liang, S. Liang, B. Liu, Y. Qian, D. K. Ji and G. Li, *Small*, 2023, **19**, 48.
- 120 N. Li, S. Gao, Y. Li, J. Liu, W. Song and G. Shen, *Nano Res.*, 2023, **16**, 7583–7592.
- 121 C. M. Tringides, N. Vachicouras, I. de Lázaro, H. Wang, A. Trouillet, B. R. Seo, A. Elosegui-Artola, F. Fallegger, Y. Shin, C. Casiraghi, K. Kostarelos, S. P. Lacour and D. J. Mooney, *Nat. Nanotechnol.*, 2021, **16**, 1019–1029.
- 122 D. Wang, D. Zhang, Q. Pan, T. Wang and F. Chen, *Sens. Actuators, B*, 2022, **371**, 132481.

- 123 P. Li, Q. Hao, J. Liu, D. Qi, H. Gan, J. Zhu, F. Liu, Z. Zheng and W. Zhang, *Adv. Funct. Mater.*, 2021, **32**, 2108261.
- 124 H. Wang, Z. Li, Z. Liu, J. Fu, T. Shan, X. Yang, Q. Lei, Y. Yang and D. Li, *J. Mater. Chem. C*, 2022, **10**, 1594–1605.
- 125 S. Zhang, X. Lin, J. Wan, C. Xu and M. Han, *Adv. Mater. Technol.*, 2024, 2301895.
- 126 C. Xu, J. Chen, Z. Zhu, M. Liu, R. Lan, X. Chen, W. Tang, Y. Zhang and H. Li, *Small*, 2023, **20**, 2306655.
- 127 D. Wang, D. Zhang, X. Chen, H. Zhang, M. Tang and J. Wang, *Nano Energy*, 2022, **102**, 107711.
- 128 W. Du, Z. Li, Y. Zhao, X. Zhang, L. Pang, W. Wang, T. Jiang, A. Yu and J. Zhai, *Chem. Eng. J.*, 2022, **446**, 137268.
- 129 S. Honda, R. Tanaka, G. Matsumura, N. Seimiya and K. Takei, *Adv. Funct. Mater.*, 2023, **33**, 44.
- 130 M. Lin, Z. Zheng, L. Yang, M. Luo, L. Fu, B. Lin and C. Xu, *Adv. Mater.*, 2021, **34**, 2107309.
- 131 W. Wu, L. Li, Z. Li, J. Sun and L. Wang, *Adv. Mater.*, 2023, **35**, 2304596.
- 132 D. Wang, D. Zhang, Y. Yang, Q. Mi, J. Zhang and L. Yu, *ACS Nano*, 2021, **15**, 2911–2919.
- 133 J. Li, J. Yin, M. G. V. Wee, A. Chinnappan and S. Ramakrishna, *Adv. Fiber Mater.*, 2023, **5**, 1417–1430.
- 134 L. Gao, C. Zhu, L. Li, C. Zhang, J. Liu, H.-D. Yu and W. Huang, *ACS Appl. Mater. Interfaces*, 2019, **11**, 25034–25042.
- 135 J.-S. Kim, Y. So, S. Lee, C. Pang, W. Park and S. Chun, *Carbon*, 2021, **181**, 169–176.
- 136 T. Yuwen, D. Shu, H. Zou, X. Yang, S. Wang, S. Zhang, Q. Liu, X. Wang, G. Wang, Y. Zhang and G. Zang, *J. Nanobiotechnol.*, 2023, **21**, 320.
- 137 F. Gao, C. Liu, L. Zhang, T. Liu, Z. Wang, Z. Song, H. Cai, Z. Fang, J. Chen, J. Wang, M. Han, J. Wang, K. Lin, R. Wang, M. Li, Q. Mei, X. Ma, S. Liang, G. Gou and N. Xue, *Microsyst. Nanoeng.*, 2023, **9**, 2–21.
- 138 C. Zhao, X. Li, Q. Wu and X. Liu, *Biosens. Bioelectron.*, 2021, **188**, 113270.
- 139 J. Tu, J. Min, Y. Song, C. Xu, J. Li, J. Moore, J. Hanson, E. Hu, T. Parimon, T.-Y. Wang, E. Davoodi, T.-F. Chou, P. Chen, J. J. Hsu, H. B. Rossiter and W. Gao, *Nat. Biomed. Eng.*, 2023, **7**, 1293–1306.
- 140 Q. Ning, S. Feng, Q. Sun, R. Yu, T. Li, H. Xu, D. Cui and K. Wang, *Nano Res.*, 2023, **17**, 3096–3106.
- 141 J. Li and X. Bo, *J. Hazard. Mater.*, 2022, **423**, 127014.
- 142 Y. Zhao, K. Q. Jin, J. D. Li, K. K. Sheng, W. H. Huang and Y. L. Liu, *Adv. Mater.*, 2023, 2305917.
- 143 Y. L. Liu and W. H. Huang, *Angew. Chem., Int. Ed.*, 2020, **60**, 2757–2767.
- 144 X. Ma, Y. Qi, Y. Niu, Q. Zhang, X. Xiang, K. Zhang, P. He, Y. Dai, W. Niu and X. Zhang, *Nano Energy*, 2023, **111**, 108424.
- 145 J. Zhao, J. Deng, W. Liang, L. Zhao, Y. Dong, X. Wang and L. Lin, *Compos. Sci. Technol.*, 2022, **227**, 109606.
- 146 K. Xia, W. Wu, M. Zhu, X. Shen, Z. Yin, H. Wang, S. Li, M. Zhang, H. Wang, H. Lu, A. Pan, C. Pan and Y. Zhang, *Sci. Bull.*, 2020, **65**, 343–349.
- 147 R. Zhao, Z. Gu, P. Li, Y. Zhang and Y. Song, *Adv. Mater. Technol.*, 2021, **7**, 2101124.
- 148 Y. Tang, P. Jin, Y. Wang, D. Li, Y. Chen, P. Ran, W. Fan, K. Liang, H. Ren, X. Xu, R. Wang, Y. Yang and B. Zhu, *Nat. Commun.*, 2023, **14**, 4961.
- 149 J. Zhong, X. Wu, S. Lan, Y. Fang, H. Chen and T. Guo, *ACS Photonics*, 2018, **5**, 3712–3722.
- 150 T. Wang, D. Zheng, K. Vegso, N. Mrkyvkova, P. Siffalovic and T. Pauporté, *Adv. Funct. Mater.*, 2023, **33**, 2304659.
- 151 T. Wang, Y. Guo, P. Wan, H. Zhang, X. Chen and X. Sun, *Small*, 2016, **12**, 3748–3756.
- 152 Y. Jin, M. Yu, D. T. Nguyen, X. Yang, Z. Li, Z. Xiong, C. Li, Y. Liu, Y. L. Kong and J. S. Ho, *npj Flexible Electron.*, 2024, **8**, 10.
- 153 D. Wang, D. Zhang and Q. Mi, *Sens. Actuators, B*, 2022, **350**, 130830.
- 154 Y. Huang, F. Yang, S. Liu, R. Wang, J. Guo and X. Ma, *Research*, 2021, **2021**, 13.
- 155 M. G. Stanford, K. Yang, Y. Chyan, C. Kittrell and J. M. Tour, *ACS Nano*, 2019, **13**, 3474–3482.
- 156 M. Zhang, K. Liu, J. Xu, P. Wang, J. Sun, W. Ding, C. Wang and K. Zhang, *ACS Sens.*, 2022, **7**(9), 2634–2644.
- 157 D. Wang, D. Zhang, J. Guo, Y. Hu, Y. Yang, T. Sun, H. Zhang and X. Liu, *Nano Energy*, 2021, **89**, 106410.
- 158 Y. Zhang, H.-X. Mei, Y. Cao, X.-H. Yan, J. Yan, H.-L. Gao, H.-W. Luo, S.-W. Wang, X.-D. Jia, L. Kachalova, J. Yang, S.-C. Xue, C.-G. Zhou, L.-X. Wang and Y.-H. Gui, *Coord. Chem. Rev.*, 2021, **438**, 213910.
- 159 W. Zhao, M. Jiang, W. Wang, S. Liu, W. Huang and Q. Zhao, *Adv. Funct. Mater.*, 2020, **31**, 2009136.
- 160 F. Lin, P. Yang, Q. Wang, Y. Zhang, W. Wang, S. Liu, W. Zhao and Q. Zhao, *Adv. Mater. Technol.*, 2023, **8**, 2300972.
- 161 K. Xu, *Natl. Sci. Rev.*, 2017, **4**, 19–20.
- 162 X. Xia, J. Yang, Y. Liu, J. Zhang, J. Shang, B. Liu, S. Li and W. Li, *Adv. Sci.*, 2022, **10**, 2204875.
- 163 H. Liu, W. Xie, Z. Huang, C. Yao, Y. Han and W. Huang, *Small Methods*, 2021, **6**, 2101116.
- 164 R. Pathak, K. Chen, F. Wu, A. U. Mane, R. V. Bugga, J. W. Elam, Q. Qiao and Y. Zhou, *Energy Storage Mater.*, 2021, **41**, 448–465.
- 165 J. Zhao, J. Zha, Z. Zeng and C. Tan, *J. Mater. Chem. A*, 2021, **9**, 18887–18905.
- 166 Y. Xu, Z. Lin, W. Wei, Y. Hao, S. Liu, J. Ouyang and J. Chang, *Nano-Micro Lett.*, 2022, **14**, 117.
- 167 Z. Li, Y. Gao, H. Huang, W. Wang, J. Zhang and Q. Yu, *Composites, Part B*, 2023, **258**, 110712.
- 168 C. Xu, Y. Niu, V. Ka-Man Au, S. Gong, X. Liu, J. Wang, D. Wu and Z. Chen, *J. Energy Chem.*, 2024, **89**, 110–136.
- 169 L. Zhao and Z. Qu, *J. Energy Chem.*, 2022, **71**, 108–128.
- 170 W. Liu, Y. Liu, Z. Yang, C. Xu, X. Li, S. Huang, J. Shi, J. Du, A. Han, Y. Yang, G. Xu, J. Yu, J. Ling, J. Peng, L. Yu, B. Ding, Y. Gao, K. Jiang, Z. Li, Y. Yang, Z. Li, S. Lan, H. Fu, B. Fan, Y. Fu, W. He, F. Li, X. Song, Y. Zhou, Q. Shi, G. Wang, L. Guo, J. Kang, X. Yang, D. Li, Z. Wang, J. Li, S. Thoroddsen, R. Cai, F. Wei, G. Xing, Y. Xie, X. Liu, L. Zhang, F. Meng, Z. Di and Z. Liu, *Nature*, 2023, **617**, 717–723.

- 171 X. Shu, Q. Chen, M. Yang, M. Liu, J. Ma and J. Zhang, *Adv. Energy Mater.*, 2022, **13**, 2202871.
- 172 K.-H. Choi, J. Yoo, C. K. Lee and S.-Y. Lee, *Energy Environ. Sci.*, 2016, **9**, 2812–2821.
- 173 T. Liu, R. Yan, H. Huang, L. Pan, X. Cao, A. deMello and M. Niederberger, *Adv. Funct. Mater.*, 2020, **30**, 2004410.
- 174 H. Wang, J. Fu, C. Wang, R. Zhang, Y. Yang, Y. Li, C. Li, Q. Sun, H. Li and T. Zhai, *Adv. Funct. Mater.*, 2021, **31**, 2102284.
- 175 I. Hussain, C. Lamiel, S. Sahoo, M. S. Javed, M. Ahmad, X. Chen, S. Gu, N. Qin, M. A. Assiri and K. Zhang, *Nano-Micro Lett.*, 2022, **14**, 199.
- 176 B. Joshi, E. Samuel, Y.-I. Kim, A. L. Yarin, M. T. Swihart and S. S. Yoon, *Coord. Chem. Rev.*, 2022, **460**, 214466.
- 177 Z. Sun, K. Qu, Y. You, Z. Huang, S. Liu, J. Li, Q. Hu and Z. Guo, *J. Mater. Chem. A*, 2021, **9**, 7278–7300.
- 178 K. Li, X. Liu, S. Chen, W. Pan and J. Zhang, *J. Energy Chem.*, 2019, **32**, 166–173.
- 179 G. Schiavone, X. Kang, F. Fallegger, J. Gandar, G. Courtine and S. P. Lacour, *Neuron*, 2020, **108**, 238–258.
- 180 X. Wang, X. Sun, D. Gan, M. Soubrier, H.-Y. Chiang, L. Yan, Y. Li, J. Li, S. Yu, Y. Xia, K. Wang, Q. Qin, X. Jiang, L. Han, T. Pan, C. Xie and X. Lu, *Matter*, 2022, **5**, 1204–1223.
- 181 B. Ji, C. Ge, Z. Guo, L. Wang, M. Wang, Z. Xie, Y. Xu, H. Li, B. Yang, X. Wang, C. Li and J. Liu, *Biosens. Bioelectron.*, 2020, **153**, 112009.
- 182 M. Xin, T. Yu, Y. Jiang, R. Tao, J. Li, F. Ran, T. Zhu, J. Huang, J. Zhang, J. H. Zhang, N. Hu, W. Wang, Q. Zhang, Z. Liu, X. Wang, Y. Shi and L. Pan, *SmartMat*, 2022, **4**, e1157.
- 183 X. Fu, L. Wang, L. Zhao, Z. Yuan, Y. Zhang, D. Wang, D. Wang, J. Li, D. Li, V. Shulga, G. Shen and W. Han, *Adv. Funct. Mater.*, 2021, **31**, 2010533.
- 184 R. Lycke, R. Kim, P. Zolotavin, J. Montes, Y. Sun, A. Koszeghy, E. Altun, B. Noble, R. Yin, F. He, N. Totah, C. Xie and L. Luan, *Cell Rep.*, 2023, **42**, 112554.
- 185 J. Li, Y. Liu, L. Yuan, B. Zhang, E. S. Bishop, K. Wang, J. Tang, Y.-Q. Zheng, W. Xu, S. Niu, L. Beker, T. L. Li, G. Chen, M. Diyaolu, A.-L. Thomas, V. Mottini, J. B. H. Tok, J. C. Y. Dunn, B. Cui, S. P. Paşca, Y. Cui, A. Habtezion, X. Chen and Z. Bao, *Nature*, 2022, **606**, 94–101.
- 186 M. Zhang, A. Pal, X. Lyu, Y. Wu and M. Sitti, *Nat. Mater.*, 2024, **23**, 560–569.
- 187 X. Guo, X. Lu, P. Jiang and X. Bao, *Adv. Mater.*, 2024, 2313911.